

MAGNETIC FIELD DIFFUSION IN SELF-CONSISTENTLY TURBULENT ACCRETION DISKS

J. HEYVAERTS

Observatoire de Strasbourg, Université Louis Pasteur, 11 rue de l'Université, 67000 Strasbourg, France;
 heyvaert@astro.u-strasbg.fr

E. R. PRIEST

St. Andrews University, Mathematical and Computational Department, North Haugh, St. Andrews, KY169SS, UK;
 eric@dcs.st-and.ac.uk

AND

A. BARDOU

Observatoire de Strasbourg, 11 rue de l'Université, 67000 Strasbourg, France; bardou@astro.u-strasbg.fr

Received 1995 November 27; accepted 1996 June 26

ABSTRACT

We show how the level of turbulence in accretion disks can be derived from a self-consistency requirement that the associated effective viscosity should match the instantaneous accretion rate. This method is applicable when turbulence has a direct energy cascade. Only limited information on the origin and properties of the turbulence, such as its injection scale and anisotropy, is needed. The method is illustrated by considering the case of turbulence originating from the magnetic shearing instability. The corresponding effective kinematic viscosity coefficient is shown to scale as the $1/3$ power of surface mass density at a given radius in optically thick disks, and to be describable by a Shakura-Sunyaev law with $\alpha \approx 0.04$. Mass flow in disks fed at a localized hot spot is calculated for accretion regimes driven by such turbulence, as well as passive magnetic field diffusion and dragging. An important result of this analysis is that thin disks supported by turbulence driven by the magnetic shearing instability, and more generally any turbulence with injection scale of order of the disk thickness, are very low magnetic Reynolds number systems. Turbulent viscosity-driven solutions with negligible field dragging and no emission of cold winds or jets are natural consequences of such regimes. Disks of accreting objects that are magnetized enough to be shielded by a magnetopause, however, may not operate in their innermost regions in the magnetic shearing instability regime. The possibility therefore remains to be explored of centrifugally driven winds emanating from such regions.

Subject headings: accretion, accretion disks — diffusion — MHD — stars: mass loss — turbulence

1. INTRODUCTION

1.1. Role of Turbulence in Accretion Disks

Accretion or collapse of material usually requires the loss of considerable amounts of angular momentum. Several physical processes that might be effective in this transport have been considered in the literature. Turbulence in an accretion disk is one such possibility, another being the escape of angular momentum in a magnetized rotating magnetohydrodynamic (MHD) wind.

Molecular or radiative viscosity is insufficient to transfer angular momentum on an adequate timescale. However, it is conceivable that, due to the high value of the Reynolds number, the flow is turbulent and that associated transport mechanisms operate. The origin of the turbulence is still uncertain. The variation with distance of the specific angular momentum in a Keplerian disk is linearly stable, but the flow might be unstable to finite-amplitude disturbances and develop turbulence by the mere effect of differential rotation (Zahn 1991; Dubrulle & Knobloch 1992). Alternative possibilities are the development of turbulence from convection (Lin & Papaloizou 1980) or from the magnetic shearing instability (Balbus & Hawley 1991; Hawley & Balbus 1991).

In the past few years, the effect of turbulent transport on the large-scale dynamics of accretion disks has usually been represented by an effective “eddy” viscosity. Transport by

eddies of small Rossby number or size larger than the disk thickness, which are subject to the Coriolis force and suffer two-dimensional dynamics, cannot be represented by effective local transport coefficients. Whether such large eddies indeed develop remains an important issue to discuss in the future. In this paper we restrict our investigation to situations in which local diffusive transport is an adequate representation. It is encouraging to note that this assumption is not grossly contradicted when turbulence is driven by hydrodynamical shear (Dubrulle 1992), and it seems also fair enough in the case of magnetic shearing instability.

In most earlier approaches, the effective viscosity has been parameterized on the basis of an interesting, but bold, argument, namely, that eddies should not be much larger than the disk half-thickness h and that their motions should not be very supersonic, for otherwise shocks would regulate the plasma temperature and the velocity of turbulent motions to almost sonic velocities. This qualitative argument is not entirely convincing, since the feeding of turbulence by accretion might enforce a supersonic regime. Nevertheless, it led Shakura & Sunyaev (1973) to propose the well-known parameterization, according to which the effective kinematic viscosity coefficient ν_t is written as

$$\nu_t = \alpha H c_s, \quad (1)$$

where H is the disk total thickness, $H = 2h$. Their argument implies that α should be of order unity, whereas actual disk

models compare favorably with observations for lower α values of the order of 0.1 (Duschl 1989). Therefore, the limitation to sonic velocities by shocks is not physically reasonable, and the above reasoning loses some of its strength. Turbulence seems actually to be subsonic. Equation (1) may still be regarded as a change of variable, however, with the representation of viscosity passing from ν_t to α ; but better arguments, giving more precise clues to the value of α , are desirable.

Several authors have attempted to elaborate on this theme. The general purpose of their approaches has been to incorporate in the disk model enough physics of the turbulence that the value of the effective viscosity would result from the model, rather than be assumed. Dubrulle (1992) proposes a modeling of turbulence in terms of relations that express the third-order moments of fluctuating quantities in terms of Reynolds stresses, which are second-order moments of the turbulent velocity. The choice of appropriate relations is inspired from an ansatz used successfully in modeling turbulent shear flows in geophysical and laboratory situations. Her modeling contains a few arbitrary coefficients, but the main uncertainty rests on the appropriate length scale of the turbulence, which implies that the nature of its source needs to be made precise. In the case of shear-driven turbulence, the scale of the largest turbulent eddies is found to be of the order of the disk thickness and is on the verge of being affected by the Coriolis force (Rossby number of order one). Duschl (1989) used mixing-length theory to calculate self-consistent disk models in which the turbulence is due to convection in convectively unstable regions of the disk. Elsewhere, another form of turbulence is assumed to be present, which is still parameterized by equation (1). More recently, Goldman & Wandel (1995) have also discussed convection-driven turbulence, representing its effects by an effective viscosity and using a phenomenological model of turbulence by Canuto, Goldman, & Chasnov (1987). They assume that the size of the largest eddies, which determines the actual effective viscosity, equals the thickness of the disk, and they take account of their anisotropy by a parameter. Though these approaches are different, their common goal is to deduce in a self-consistent manner the turbulence level in the disk.

Any closure model of disk turbulence has to provide the means to determine the constants that enter the theory, or else to accept them as free parameters of the representation. Often these constants have to be determined a posteriori by calibrating the model with real experimental or numerical results. Our approach is also of this general type. The turbulence that develops is characterized by its injection scale, the most appropriate value of which is discussed on the basis of physical arguments below, but it is not deduced mathematically. Indeed, this injection scale, a concept itself of limited relevance since in reality there is likely to be an injection range, must depend on the nature of the instability feeding the turbulence. Therefore, this paper pays special attention to the case in which turbulence is driven by the magnetic shearing instability, since it may indeed be the source of turbulence, but the philosophy of determining self-consistently some of the properties of the turbulence spectrum is of more general relevance. Indeed, our approach introduces a macroscopic self-consistency argument to determine the level to which the turbulence builds up at each point in the disk: namely, that the turbulence level must be consistent with the instantaneous dissipation

that necessarily accompanies accretion. Such a self-consistency argument, discussed also by Zahn (1991), is of quite general validity. It is very useful because it makes the effective viscosity a function of the macroscopic properties of the flow, and, within the limits of validity of the α -model, which this approach partly justifies, it would give conceptually the value of α . In practice, though, several uncertainties and difficulties do not make it possible to reach this goal quantitatively. Let us stress again that the identification of the effective viscosity as that coefficient that appears in the rate of dissipation of mechanical energy with the one that appears in the momentum transport contains an implicit assumption on the nature of turbulent transport. It assumes that the turbulent eddies that cause the effective momentum transport are small enough for the transport to be describable by effective transport coefficients and that they suffer a direct energy cascade, so that momentum transport indeed results in associated dissipation.

Particular attention is given in this paper to the case in which turbulence in the disk is fed by the magnetic shearing instability (Balbus & Hawley 1991). When dealing with this instability, we should take into account the effect of anisotropies induced by differential rotation and partial two-dimensionality, which is an important aspect revealed by recent numerical calculations. This introduces further parameters in the theory, some of which may be reasonably chosen, but not determined precisely, by consideration of recent results of numerical simulations relevant to this instability.

The shape of the spectrum is taken to be a power law and is subject to the condition that its small wavenumber cutoff in the vertical direction be larger than π/h . Limitations that result from assumptions on the shape of the spectrum are less serious than those that result from uncertainties concerning the turbulence characteristic scale and the role of two-dimensional horizontal eddies, if any. Such difficulties are implicit or explicit in any existing attempt to construct self-consistent turbulent disk models. The effective viscosity is dominated by the largest scales present in the spectrum, so that its precise shape, Kolmogoroff or otherwise, is of secondary importance, since spectral shape parameters enter as numerical factors of order unity in the final results. The actual value of the small wavenumber cutoff and spectrum anisotropies may have more serious numerical consequences.

We discuss turbulence-feeding mechanisms and the associated injection scale, which support the idea that, at least in weakly magnetized accretion disks, the turbulence is dominated by scale lengths of the order of the local disk thickness. Then we illustrate, by showing a few explicit solutions, how mass spreads in the process of accretion in the presence of such a self-consistent viscosity. Finally, we turn to the question of passive magnetic field diffusion through thin turbulent disks.

1.2. *Magnetic Field Diffusion in Accretion Disks*

Magnetic field expulsion from collapsing matter has been a long-standing (Mestel 1966; Mestel & Strittmatter 1967) and important problem, since a gas cloud could only suffer gravitational instability if the mass to magnetic flux ratio exceeds a limit that is usually not reached initially in the interstellar medium. Indeed, the mass to flux ratio of newly born stars appears to be much larger than that of parent clouds.

The evolution of this ratio in star-forming clouds can be driven by restrictive field diffusion, as considered first by Mestel (1966) and Mestel & Strittmatter (1967), or by ambipolar diffusion, as suggested by Mestel & Spitzer (1956) and developed later in some detail by many authors, in particular Nakano (1979), Lizano & Shu (1989), Fiedler & Mouschovias (1992), and Mouschovias & Morton (1992). Ambipolar diffusion occurs in weakly ionized media and operates most effectively in the cool, dense cores of molecular clouds. Its effect (Fiedler & Mouschovias 1992) is to redistribute flux in the cloud in such a way that a central portion of it becomes supercritical against the magnetic Jeans instability and eventually collapses, while the envelope remains magnetically supported (Mouschovias 1995). Ambipolar diffusion may be helped at large neutral densities by the plasma microinstabilities that develop in weakly ionized media (Norman & Heyvaerts 1985). Altogether, star formation by ambipolar diffusion appears to be a low-efficiency process, since little mass eventually collapses from a much larger initial condensation. Angular momentum also has to be lost in the process of star formation. This effect is usually attributed to magnetic braking. The question should nevertheless be asked about the effect of turbulence in a condensing protostellar disk on both angular momentum loss and flux leakage.

Flux leakage and magnetic drag in accretion flows is also a problem relevant to accretion disks around young stellar objects, X-ray binaries, and active galactic nuclei. These processes control the degree of magnetization of a disk and bear on its ability to lose angular momentum in a centrifugally driven cold wind (Blandford & Payne 1982; Pudritz & Norman 1983). The problem of turbulent flux diffusion through an accretion disk has been considered recently by Lubow, Papaloizou, & Pringle (1994), who studied passive field diffusion in a resistive disk, considering the magnetic diffusivity as a parameter. We consider essentially the same problem here, but we develop a theory to obtain a more specific expression for the magnetic diffusivity, and we show that, for thin disks, the system operates necessarily in the low magnetic Reynolds number limit, provided the injection scale is not much smaller than the disk thickness. This means that the field diffuses away much faster than it is radially advected. We derive a slightly more elaborate form of the integro-differential equation that governs field diffusion in such systems and solve it analytically in the limit of low effective magnetic Reynolds numbers.

A consequence is that this type of self-consistent turbulent disk does not create favorable conditions for the emission of cold centrifugally driven winds by which they could also lose angular momentum to infinity. It seems that the two modes of angular momentum loss advocated above, i.e., turbulent viscous loss and torque from an MHD rotating magnetized wind, are unlikely to coexist in the turbulent regime associated with the magnetic shearing instability. Another consequence is that flux loss by protostellar clouds would probably be a lot more effective than anticipated from laminar disk studies if they were in a turbulence regime similar to the one described in this paper. This, however, is not certain, since the magnetic field is thought to have an energy comparable to the kinetic energy in such clouds, which makes the magnetic shearing instability somewhat more unlikely, so that the nature and level of turbulence could differ from those discussed below. We return further to this point at the end of § 2.5.

2. SELF-CONSISTENT TURBULENCE LEVEL IN ACCRETION DISKS

2.1. Self-Consistent Turbulence Level in General

That the turbulence level in an accretion disk should be a self-consistent function of mass surface density basically results from the fact that the turbulence adjusts to such a level that the mass accretion rate \dot{M} imposed by the macroscopic evolution of the system be possible. How this arises can be understood as follows. Call $\nu_*(r)$ the yet-unknown effective viscosity at radius r , the rotation law $\Omega(r)$ being Keplerian, say. The rate ϵ of viscous heating per unit mass is

$$\epsilon = \nu_*(r) d\Omega/dr)^2. \quad (2)$$

At a given radius, this heating rate ϵ determines both the vertical distribution of temperature $T(r, z)$ and the density in the disk, by vertical mechanical balance and energy balance. So, for a given mass surface density $\sigma(r)$ and a given effective viscosity $\nu_*(r)$, the local half-thickness of the disk $h(r)$ and its vertical temperature distribution are determined. This sets the stage at which the turbulence that causes the effective viscosity and dissipation is going to develop and, in fact, these macroscopic features, as we shall show, determine its level. Actually, the injection scale in this geometry has to be a function of the disk half-thickness $h(r)$, as discussed more precisely below. The effective viscosity depends both on this injection scale and on the level of turbulence, or, what is equivalent, on the rate of transfer of energy in a direct cascade, which is also just the rate of heating per unit mass, ϵ . We assume the turbulent cascade to be at any time and at any point in a stationary state (even though the global hydrodynamical system may not be). This is a reasonable assumption, since the cascade develops in a large-eddy turnover time, which is of the order of the dynamical time $1/\Omega$ and is much shorter than the matter transit time (r/v_r) . So ν_* is a function of h and ϵ , but ϵ is also related to ν_* by the “macroscopic” equation (2). Since h depends indirectly on σ and ν_* by vertical equilibrium, the turbulent viscosity will ultimately be expressed as a function of itself and σ . The solution of this self-consistency equation will eventually give ν_* in terms of σ , and of the external parameters, if any. These relations are summarized in Figure 1.

The idea that the turbulence level adapts such as to be self-consistent with large-scale constraints that ultimately cause the system to be in a turbulent state is quite general. It applies, under some weakly restrictive conditions, whatever the nature of the instability that feeds the turbulence. The general scheme described above to calculate the turbulence level works any time the effects of the turbulence can be described on the “macroscopic” scale by effective transport coefficients. This general philosophy has also been used to calculate the rate of heating in the turbulent corona of the Sun by Heyvaerts & Priest (1992) and by Inverarity, Priest, & Heyvaerts (1995). Application to the accretion disk situation is in fact easier because the nature and properties of turbulence are becoming better understood thanks to progress in numerical simulations of these systems.

In the following, we illustrate first the method in the simple case in which the turbulence develops in the system in the form of an isotropic Kolmogoroff spectrum. Then we present a calculation of the effective viscosity in the particular case of turbulence fed by the magnetic shearing instability, a situation which, for accretion disks, is probably more realistic than Kolmogoroff turbulence.

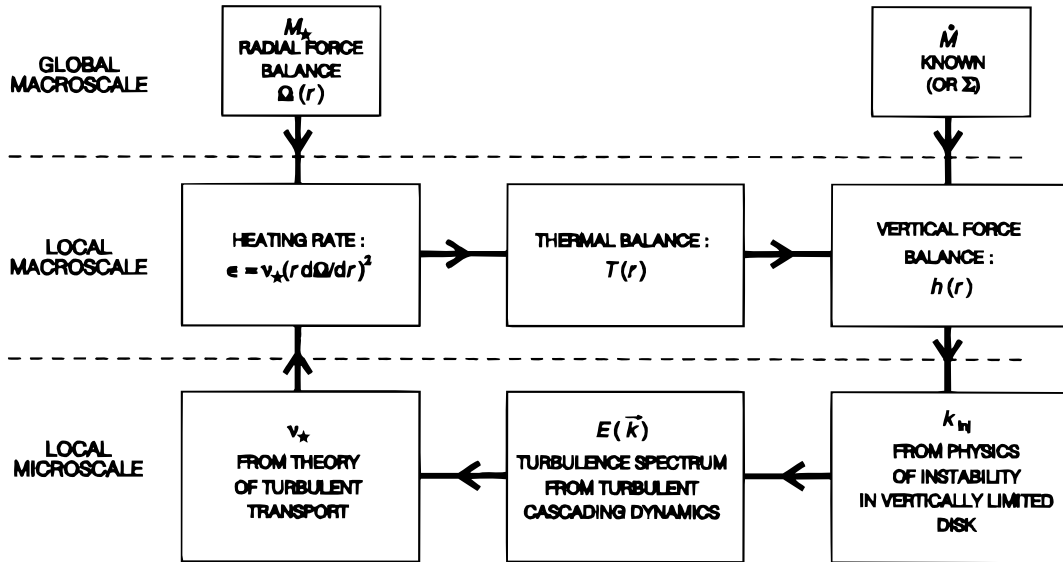


FIG. 1.—The turbulence level in a thin accretion disk is established as a result of a self-consistency process controlled by the mass of the accreting star M_* and the accretion rate \dot{M} . There is a feedback from the effective viscosity ν_* onto the local disk thickness h that partly controls the size of turbulent eddies k_{inj}^{-1} and so ν_* itself. The figure illustrates this feedback with arrows indicating the sense of the causal relations between various physical effects. The self-consistency process puts turbulent phenomena at the local microscale in relation to phenomena at the local or global macroscale.

2.2. Self-Consistency for Isotropic Kolmogoroff Turbulence

As a first illustration, consider a simple case in which turbulence locally has a Kolmogoroff spectrum given by

$$E(k) = C_K \epsilon^{2/3} k^{-5/3}. \quad (3)$$

More realistic turbulence will be considered later on. Here C_K is the Kolmogoroff constant, whose value is near 1.4, and the short wavenumber cutoff is denoted by k_{inj} . This injection scale and the rate of energy transfer in the cascade are functions of the radius r . Then, the associated effective viscosity can be written as

$$\nu_* = \lambda \epsilon^{1/3} k_{\text{inj}}^{-4/3}, \quad (4)$$

where ϵ is the usual energy transfer rate in the cascade. The dimensional part of equation (4) is simply proportional to the product $lv(l)$ of the size of the largest eddies and the typical velocity $v(l)$ associated with them, which in three-dimensional hydrodynamic turbulence is $v(l) = (2\epsilon l)^{1/3}$. Here λ is a dimensionless parameter that incorporates all the quantitative aspects of momentum transport by this turbulence spectrum. Its value is connected with the model adopted to calculate it (Moffatt 1983). This evaluation is complicated here by the fact that the turbulent medium is inhomogeneous, even vertically. Also, the concept of a sharp low-wavenumber cutoff and a precisely defined injection scale is an idealized representation, which Canuto et al. (1987) have tried to overcome by developing a technique to obtain the shape of the spectrum when cascading and injection are mixed. All these complications would affect the actual value of λ .

Therefore, we treat λ as a parameter in this paper, although it could be deduced mathematically by adopting some specific model of momentum transport by the turbulent flow. The nature of this parameter is then different from the more basic parameters, such as the injection scale, which cannot be determined precisely from the theory itself. For definiteness, we adopt the usual expression

$$\nu_* = \frac{1}{3} v l_c, \quad (5)$$

where v is the rms turbulent velocity and l_c is the correlation length. The former is given by

$$v = \left[\int_{k_{\text{inj}}}^{\infty} E(k) dk \right]^{1/2} = \sqrt{\frac{2}{3}} C_K \epsilon^{1/3} k_{\text{inj}}^{-1/3}. \quad (6a)$$

The correlation length can be defined as the weighted mean of $2\pi/k$, which gives

$$l_c = \frac{1}{v^2} \int_{k_{\text{inj}}}^{\infty} \frac{2\pi}{k} E(k) dk = \frac{4\pi}{5k_{\text{inj}}}. \quad (6b)$$

After simple calculations we obtain in this case

$$\lambda = \frac{4\pi}{15} \sqrt{\frac{3C_K}{2}}. \quad (7)$$

The eddies that make the three-dimensional part of the turbulence are not expected to be larger than the disk thickness at the considered radius. Thus, the injection scale, l_{inj} , should be a fraction $1/f$ of the total disk thickness $2h$:

$$l_{\text{inj}} = 2h/f, \quad (8a)$$

so that

$$k_{\text{inj}} = f \frac{\pi}{h}. \quad (8b)$$

Usually, f would be larger than unity. If it were to happen that eddies larger than the disk thickness are excited and still enter a direct cascade, then f might be smaller than unity. Finally, the effective viscosity is written as

$$\nu_* = \frac{\lambda}{(\pi f)^{4/3}} \epsilon^{1/3} h^{4/3}. \quad (9)$$

This can be turned into an expression for the level of turbulence (as measured by the rate of energy transfer ϵ in the cascade) in terms of the effective viscosity. Such an expres-

sion reflects only properties of the underlying turbulence. It expresses nothing more than the relation between the level and scale of the turbulence and the associated effective viscosity:

$$\epsilon = \frac{(\pi f)^4}{\lambda^3} \frac{v_*^3}{h^4}. \quad (10)$$

Now, express the fact that the rate of heating per gram, as given in terms of effective viscosity by equation (2), is just the same ϵ as in equation (10), because the power that goes into heating per gram is the energy that reaches the dissipation range of the cascade per second. A similar idea has been developed by Zahn (1991). Noting that for Keplerian rotation $r d\Omega/dr = 3\Omega/2$, we obtain by equating expressions (2) and (10)

$$\frac{9}{4} v_* \Omega^2 = \frac{(\pi f)^4}{\lambda^3} \frac{v_*^3}{h^4}. \quad (11)$$

Since h and f are implicitly functions of v_* , σ , and possibly external parameters, p say, v_* appears to be a solution of the equation

$$v_* = \frac{3\lambda^{3/2}}{2\pi^2} \frac{\Omega h^2(v_*, \sigma, p)}{f^2(v_*, \sigma, p)}. \quad (12)$$

An important aspect of such a relation is that it determines the effective viscosity self-consistently from the global properties of the large-scale flow only. Indeed, equation (12) is still no complete solution to our problem, since an expression should be obtained for $h(r)$ and $f(r)$ in terms of the surface density σ and of v_* . The profile of disk thickness with radius $h(r)$ results from mechanical balance and energy balance, and $f(r)$ is a property of the instability processes that locally feed the turbulence. Our aim in this work is to elaborate somewhat more on this connection between the actual level of turbulence and the large-scale dynamics, and to examine consequences for some MHD aspects of accretion disks, such as field dragging by the accreting matter.

2.3. Discussion of Injection Scale

We define the injection scale as the size of the eddies that carry most spectral energy density and still feed energy into a direct cascade, leading to dissipation. The physics of the instability that feeds the turbulence determines an injection scale, or an injection range.

Two-dimensional hydrodynamic turbulence does not develop direct cascades (Kraichnan & Montgomery 1980) because enstrophy can decay only in three-dimensional hydrodynamical motions. Hence, those eddies, if any, that are generated with a scale much larger than the disk thickness cannot feed a direct cascade in a purely hydrodynamical disk, but they do if the medium is embedded in a turbulent magnetic field. It is known, indeed, that homogeneous two-dimensional MHD turbulence has a direct cascade of energy and an inverse cascade of the square of the vector potential of the two-dimensional magnetic field (Fyfe, Joyce, & Montgomery 1977; Matthaeus & Montgomery 1980). The fate of two-dimensional eddies in purely hydrodynamical disks, and their effect on accretion, remain to be discussed (Dubrulle & Valdetarro 1992). The inverse cascade in a hydrodynamical disk must develop from those unstable perturbations that have a scale larger than or of

the order of the total disk thickness $2h$ or, which in practice is almost equivalent, from perturbations associated with a Rossby number smaller than unity.

Turbulence-feeding instabilities, depending on their nature, may inject energy at scales smaller or larger than $2h$. In this paper, we consider a situation in which the turbulent energy is injected at scales not much larger than the disk thickness and suffers only direct cascading.

This point of view, which cannot be of general validity, is supported by the following considerations. Our paper is concerned with field diffusion in magnetized accretion disks. Therefore, turbulence should in this case have a magnetic component. If the disk is to be MHD turbulent, and we know from the work of Balbus & Hawley (1991, 1992) that it should be, then even eddies larger than the disk thickness (if any are generated by the instability) would feed a direct energy cascade. The limitation to direct cascading that appears in hydrodynamical turbulence when the Rossby number equals unity does not apply to MHD turbulence (Dubrulle 1992).

We believe, nevertheless, that the primary excitation should be concentrated anyway in this case on scales no larger than the disk thickness scale for the following reasons. The linear stability criterion (Balbus & Hawley 1991) indicates that perturbations that are to grow from a vertical field component do so if their wavelength along the rotation axis is larger than some critical minimum value. Since the perturbation has to fit into the disk thickness, this indicates that the instability is quenched when the field exceeds a certain critical value and develops for any field smaller than the threshold. When there is instability and such a component normal to the disk is present, unstable perturbations with scale no larger than the disk thickness are generated.

The magnetic shearing instability develops also in purely azimuthal initial fields, provided it is nonaxisymmetric (Balbus & Hawley 1992; Foglizzo & Tagger 1994; Foglizzo 1994). In this case, the growth rate is reduced (Balbus & Hawley 1992), but purely toroidal fields are exceptional and constitute a singular case. Even if fields were initially like this, magnetic buoyancy (Stella & Rosner 1984; Sakimoto & Coroniti 1989) and the Parker instability, which differs from the magnetic shearing instability only by its polarization (Foglizzo 1994), should turn them into fields emerging randomly out of the disk or pushed to its periphery (Torkelsson 1993). The idealized situation would then not be maintained, and the azimuthal extent of segments of purely toroidal magnetic field lines embedded in the disk should be restricted, limiting, by lack of coherent enough space, the development of very low azimuthal wavenumber perturbations. In general, we expect actual fields to have a significant nonzero vertical component, from which perturbations with a nonzero k_z would grow. This point of view is supported entirely by the three-dimensional numerical calculations of Hawley, Gammie, & Balbus (1995).

Differential rotation in the disk has an important effect on nonaxisymmetric perturbations because such disturbances suffer strong shearing from the differentially rotating Keplerian flow, which causes the radial component of the wavevector of any convected disturbance to grow linearly in time at a rate given, for an azimuthal Fourier component of order m , by $dk_r/dt \approx (m/r)d(\Omega r)/dr$. This results in a fast secular increase of the radial wavenumber (Balbus & Hawley 1992; Foglizzo 1994), which limits the

period of wave growth, although the increase of wave amplitude remains large enough to allow us to speak of an instability. It causes low radial wavenumber perturbations to evolve into larger wavenumber ones.

To sum up, we expect the Balbus-Hawley instability mostly to feed perturbations with a wavevector larger than or equal to π/h and of course smaller than the value k_{\max} at which instability is quenched by dissipation. The injection scale for this instability, as defined above, should then be some fraction (1/2 or 1/3, say) of $2h$, even though the linearly most unstable k_z is much larger than π/h . This is because the instability acts up to $k_z = \pi/h$, so that, as time goes by, a significant noise is generated down to this wavenumber. Nevertheless, inhomogeneity effects will probably limit the growth of eddies having a vertical size exactly equal to the total disk thickness H , and we expect the actual injection scale to be somewhat smaller. Numerical calculations by Hawley et al. (1995) indeed support the point of view that the injection scale is much larger than the most linearly unstable wavelength, while in the calculations by Brandenburg et al. (1995) the vertical correlation length has been found to be of order 0.16 for a disk thickness of order 1, in a box of vertical thickness 4. This shows that, at least for the boundary conditions adopted by these authors, the dominant eddy size is not exactly the total disk thickness, but a fraction of it.

2.4. Anisotropic Spectrum for Shear-driven MHD Turbulence

Hawley et al. (1995) show that in three dimensions the magnetic shearing instability develops an anisotropic turbulence spectrum, the excitations being the largest for wavevectors such that $|k|$ is of order of the reciprocal vertical size of the computation box, which in nature would correspond to the disk thickness. They find that the extension of cells in the azimuthal direction is larger than their extension in meridional planes, which appears in wavevector space as a smaller extension of the spectrum in the k_θ -direction. Surfaces of equal spectral energy in this space are similar to flattened ellipsoids, slightly skewed in the $k_r - k_\theta$ plane, as expected for distributions that transport momentum.

These are the effects of differential rotation. Turbulence appears in the form of cells, similar in shape to rolls elongated in the θ -direction, but covering in general a part of the disk circumference only. This is still not two-dimensional turbulence because azimuthal gradients remain, and these flows have nonzero azimuthal components of field and velocity perturbations and an azimuthal field component produced by shear. The latter component couples motions in the different meridional planes.

Except for the anisotropy of the spectrum, Hawley et al. (1995) found the spectral shape not to differ very much otherwise on each of the principal axes of the wavevector space from a Kolmogoroff spectrum [for which the energy spectral power in wavevector space $W(k)$ scales as $k^{-11/3}$].

Brandenburg et al. (1995) have performed similar simulations, including effects of compressibility and stratification. They imposed boundary conditions that forbid the presence of an organized vertical magnetic field perpendicular to the disk (the vertical flux is kept equal to zero at all times, but not the azimuthal or radial flux). They too found that the turbulence develops an anisotropic spectrum, but their different boundary conditions allowed a dynamo process to develop, resulting in the generation of a rather large, but

time-oscillating, azimuthal field component with even parity in z . This component carries somewhat more energy than turbulent kinetic motions and thermal motions. Their simulation gives a smaller α value than the simulation by Hawley et al. (1995), but the reason for this is not given precisely by Brandenburg et al. (1995). It might be related to the fact that the vertical coherence scale of the magnetic field in their simulation is smaller, because the average vertical magnetic field has been constrained to vanish by Brandenburg, but not by Hawley.

2.5. Effective Viscosity of Turbulence Driven by the Magnetic Shearing Instability

In order to take into account the anisotropy of the turbulence spectrum revealed by these calculations, it is necessary to derive an expression generalizing equation (9) for such anisotropic Kolmogoroff-like spectra. Let us assume, as suggested by the numerical results, that the turbulence spectrum can be represented by a “flattened” Kolmogoroff spectrum. Such a spectrum is a function of the energy transfer rate ϵ , of the ratio q of small to large axes of ellipsoids in k -space on which the power density is assumed constant, and of a “modified” wavenumber K that parameterizes these ellipsoids:

$$K = \left(k_r^2 + k_z^2 + \frac{k_\theta^2}{q^2} \right)^{1/2}. \quad (13)$$

Turbulence would appear isotropic in the space of “modified” wavevectors K but not in real wavevector space. Modified and real wavevectors are related by $k_r = K_r$, $k_z = K_z$, $k_\theta = qK_\theta$.

It is easy to repeat in this case Kolmogoroff’s dimensional argument to find that the energy spectral power density in real wavevector space $W(k)$, which is assumed to depend only on ϵ , q , and K , must necessarily be expressible as

$$W(k) = C(q)\epsilon^{2/3}K^{-11/3}. \quad (14)$$

Since q enters as a dimensionless parameter on which the solution for the power spectrum depends, the dimensionless factor in front of the right-hand side of equation (14) depends on q and is no longer a universal constant, as in three-dimensional isotropic Kolmogoroff turbulence. Dimensional reasoning alone cannot tell how this factor depends on q . An approximate value of $C(q)$ can, however, be found by requiring that the nonlinear energy transfer time be, for eddies of any size, of order of their turnover time. This idea is consistent with the spectrum having a Kolmogoroff slope. It is a consistent assumption if the turnover time of the largest eddies is no longer than any other appropriate evolution time, which we check in the Appendix. It is found that the nonlinear transfer time given by equation (150) can be written as

$$\tau_{\text{transfer}} = \sqrt{\frac{3}{5}} [4\pi q C(q)]^{3/2} \frac{1}{K\sqrt{\langle v_k^2 \rangle}}. \quad (15)$$

By requiring that this time be of order of the eddy turnover time,

$$\tau_{\text{turn}}(K) \approx \frac{1}{K\sqrt{\langle v_k^2 \rangle}}, \quad (16)$$

it is found that $4\pi q C(q)$ should be of order unity. For isotropic turbulence, which corresponds to $q = 1$, the quan-

tity $4\pi C(1)$ equals the Kolmogoroff constant C_K which is indeed of order unity. Here, however, the anisotropy parameter q is not close to unity because the wavevectors that carry the largest excitation should have k_z of order π/h , not very different from their radial wavenumbers, while their azimuthal wavelength would be a fraction of the circumference of a circle of radius r . So q should be of order $h(r)/r$. The value (of order unity) of $4\pi q C(q)$ in this regime is then uncertain. For definiteness, we assume

$$4\pi q C(q) = 1, \quad (17)$$

while our reasoning implies only a value of order unity. The effective viscosity can then be deduced as in § 2.2. This gives

$$\nu_* = \frac{2\pi^2}{15} \sqrt{\frac{3}{2}} \epsilon^{1/3} k_{\text{inj}}^{-4/3}, \quad (18)$$

identifying a specific value of the parameter λ introduced in equation (4), namely,

$$\lambda = \frac{2\pi^2}{15} \sqrt{\frac{3}{2}}. \quad (19)$$

As discussed in the preceding paragraph, the injection scale for the magnetic shearing instability appears to be a fraction of the total disk thickness $2h$ so that the injection wavenumber k_{inj} is $f\pi/h$, with f of order a few. To be specific, let us adopt

$$f = 2. \quad (20)$$

Then the effective viscosity in turbulence driven by the magnetic shearing instability is given by equation (12), with $f = 2$ approximately and λ given approximately by equation (19).

This can be translated into a value of the Shakura-Sunyaev parameter α . Comparing equation (1) with equation (12), taking into account that $H = 2h$, $\Omega h = c_s$ (eq. [28] below), $f = 2$, and that λ is given by equation (19), we find that

$$\alpha = \frac{3\lambda^{3/2}}{4\pi^2 f^2} = \frac{3}{16\pi^2} \left(\frac{2\pi^2}{15} \sqrt{\frac{3}{2}} \right)^{3/2} = 0.04. \quad (21)$$

Note that this value is still subject to uncertainties in the actual value of λ (since eq. [17] is but an estimate) and that the actual value of f need not be exactly 2. Only numerical calculations carried out with representative boundary conditions would make it possible to ascertain more precisely the values of λ and f . We believe, however, that the figures adopted in equations (17) and (20) should not be uncertain by more than a factor of approximately 2. This view is indeed supported by the fact that the recent numerical simulations by Stone et al. (1996), which take into account the vertical stratification of the disk, a key aspect in our view, indeed lead to numerically observed α -values of order 10^{-2} , as implied by equation (21).

2.6. Consequences of Limitations to the Magnetic Shearing Instability

When the vertical component of the magnetic field becomes too large, the development of the magnetic shearing instability is inhibited. This is because the instability can grow only for vertical wavelengths larger than a certain

minimum value: otherwise the restoring magnetic tension force exceeds the destabilizing centrifugal and gravitational forces. When this minimum wavelength becomes equal to the disk thickness, the instability is quenched. This happens (Balbus & Hawley 1991) for a vertically isothermal disk when the ratio of gas pressure to magnetic pressure associated with the field component perpendicular to the disk drops below $\pi^2/3$, i.e., becomes of order unity. This is a rather stringent condition, which is likely to be met only in the regions of a disk that are near the accreting object, if the latter is a sufficiently magnetized object. The pressure exerted by a field having its sources in remote objects is likely to be much smaller than the gas pressure. When the field has become strong enough that this situation is realized, the magnetic field rigidity is large enough to two-dimensionalize the turbulent motions in the disk, if they remain subsonic. The problem of turbulent development in disks would then be posed in entirely different terms. We do not consider such a situation further in this paper.

It is interesting, though, to speculate on its possible consequences. First, let us suppose that the flow is no longer turbulent. Then nonlinear instabilities would remain a possible source of developing perturbations, as well as several unstable situations that have been identified for strongly magnetized disks of negligible thickness. Among them, we should quote the magnetic interchange instability discussed by Spruit & Taam (1990), Lepeltier & Aly (1996), and Lubow & Spruit (1995) and more recently by Spruit, Stehle, & Papaloizou (1995), and the spiral wave instability of magnetized disks discussed by Tagger et al. (1990). The magnetic interchange instability occurs if the field decreases with distance to the axis, and only if there is a deviation from Keplerian rotation due to the radial component of Lorentz forces, so that the plasma is partly supported by the field. This means that the instability operates only near the disk-magnetosphere interface. Spruit et al. (1995) have shown that such an instability operates in the quasi-incompressible regime, and only in those regions in which the field is dynamically significant. This means that $B^2/(2\mu_0)$ must be of the order of a fraction of ρv^2 . By comparison, the Balbus-Hawley instability is quenched when the magnetic energy density becomes comparable to the thermal energy density ρc_s^2 , where c_s is the sound speed. From the work of Tagger et al. (1990), it is known that spiral magnetosonic waves grow unstable due to differential rotation by the swing mechanism. The favored azimuthal wavelength varies with the degree of magnetization. At the radius of the disk at which the magnetic shearing instability ceases to operate (i.e., where the Alfvén speed and sound speed become comparable), this most unstable wavelength is of the order of the disk thickness, but it becomes much larger in the region between this radius and the magnetopause, where the degree of magnetization becomes larger. So the turbulence that might develop in this region if there is such a region as a result of such instabilities would consist of two-dimensional vortices on a scale larger than the disk thickness. It is not certain that any description of their effects in terms of local transport would still be appropriate. If the magnetic field that threads the disk is not open but anchored in the accreting star, the random motion of field footpoints in the disk would braid the field lines in the region between disk and star, which would lead to some heating of the tenuous medium in this region by a mechanism similar to that which has been suggested to operate in

the solar corona (Parker 1983; van Ballegooijen 1986; Heyvaerts 1990).

2.7. Effective Viscosity as a Function of Surface Mass Density

Adopting the results of equations (19) and (20), the value of the effective viscosity becomes quite definite, and equation (12) can be written as

$$\nu_* = \frac{3\lambda^{3/2}}{8\pi^2} \Omega h^2, \quad (22)$$

where λ is given by equation (19) and $f = 2$. In order to turn equation (41) into one for the effective viscosity, we need to solve for the vertical force balance and the energetics. This will eventually give the disk thickness in terms of the effective viscosity and surface mass density Σ and then ν_* as a function of Σ . Before actually doing this, it is useful to switch to dimensionless quantities. Adopting some reference radius R_0 as a unit of length and the associated Keplerian period in the field of the accreting mass M_* as a reference time, the natural reference value for diffusion coefficients is

$$\nu_{*0} = R_0^2 \sqrt{\frac{GM_*}{R_0^3}}. \quad (23)$$

The dimensionless viscosity ν is therefore defined as

$$\nu_* = \nu_{*0} \nu, \quad (24)$$

where from equation (22)

$$\nu = \frac{3\lambda^{3/2}}{8\pi^2} \left(\frac{R_0}{r}\right)^{3/2} \left(\frac{h^2}{R_0^2}\right). \quad (25)$$

Let us now introduce some simplifying assumptions concerning the vertical force balance and energy balance. The plasma is assumed to be fully ionized hydrogen. The free particle number density is n , and the mass density is $\rho = nm$, m being the average mass per free particle, $(m_p + m_e)/2$. The equation of state is taken to be that of a perfect gas,

$$p = nk_B T, \quad (26)$$

where k_B is the Boltzmann constant. The disk is assumed to be optically thick and isothermal in the vertical direction. This is a reasonable assumption because heat is efficiently transported vertically by turbulent motions with eddy size of order of the disk thickness.

The vertical force balance between a pressure gradient and the vertical part of the gravitational force exerted by the central star (we do not consider self-gravitating disks) can then be solved easily, giving

$$n(r, z) = n_0(r) \exp\left(-\frac{GM_* m z^2}{2k_B T r^3}\right). \quad (27)$$

This identifies the disk half-thickness $h(r)$ as

$$h^2(r) = \frac{2k_B T(r)r^3}{GM_* m}. \quad (28)$$

To find the temperature $T(r)$, we need to solve the energy equation. Neglecting the kinetic energy associated with the radial and vertical components of the velocity, as well as the thermal energy density and the enthalpy flux, which are

small in thin disks, the height-integrated form of the energy equation is

$$\begin{aligned} & \frac{\partial}{\partial t} \left[\Sigma \left(\frac{\Omega^2 r^2}{2} - \frac{GM_*}{r} \right) \right] + \frac{1}{r} \frac{\partial}{\partial r} \\ & \times \left\{ r \left[\Sigma v \left(\frac{\Omega^2 r^2}{2} - \frac{GM_*}{r} \right) - \nu_* \Sigma r^2 \Omega \frac{\partial \Omega}{\partial r} \right] \right\} = -2 \sigma_B T^4. \end{aligned} \quad (29)$$

In this equation, σ_B is the Stefan-Boltzmann constant. The last term in the divergence is the viscous energy flux, while the right-hand side of equation (29) represents losses by blackbody radiation through the upper and lower faces of a circular strip between r and $r + dr$. Radial force balance between gravity and centrifugal forces imposes a Keplerian azimuthal velocity. Using mass conservation, equation (29) then takes the form

$$\begin{aligned} & \frac{GM_*}{2} \left[\frac{\partial \Sigma}{\partial t} + \frac{1}{r} \frac{\partial}{\partial r} (r \Sigma v) \right] + r \Sigma v \frac{\partial}{\partial r} \left(\frac{GM_*}{2r} \right) \\ & + \frac{\partial}{\partial r} \left(\nu_* \Sigma r^3 \Omega \frac{\partial \Omega}{\partial r} \right) = 2r \sigma_B T^4. \end{aligned} \quad (30)$$

The angular momentum conservation equation is deduced from the azimuthal component of the equation of motion by multiplying it by r . It can be written as

$$\frac{\partial}{\partial t} (\Sigma r^2 \Omega) + \frac{1}{r} \frac{\partial}{\partial r} \left[r \left(r^2 \Omega \Sigma v - \nu_* \Sigma r^2 \frac{\partial \Omega}{\partial r} \right) \right] = 0. \quad (31)$$

For a time-independent Ω , as is the case for Keplerian rotation, it can be manipulated, using mass conservation, into the form

$$\Sigma v \frac{\partial}{\partial r} (r^2 \Omega) - \frac{1}{r} \frac{\partial}{\partial r} \left(\nu_* \Sigma r^3 \frac{\partial \Omega}{\partial r} \right) = 0. \quad (32)$$

Multiplying by Ω , we obtain an expression for the viscous flux that appears in equation (30), namely,

$$\frac{1}{r} \frac{\partial}{\partial r} \left(\nu_* \Sigma r^3 \Omega \frac{\partial \Omega}{\partial r} \right) = \nu_* \Sigma r^2 \left(\frac{\partial \Omega}{\partial r} \right)^2 + \Sigma v \Omega \frac{\partial}{\partial r} (r^2 \Omega). \quad (33)$$

Substituting this in equation (30), we finally obtain, for Keplerian rotation,

$$\sigma_B T^4 = \frac{9}{8} \frac{\nu_* \Sigma}{r^2} \frac{GM_*}{r}. \quad (34)$$

Let us introduce also a dimensionless form of the mass surface density σ by introducing a reference mass M_0 , of the order of the disk mass

$$\Sigma = \sigma \frac{M_0}{R_0^2}, \quad (35)$$

in terms of which the temperature obtained in equation (34) can be expressed as

$$T^4(r) = \left(\frac{9GM_* M_0}{8 \sigma_B R_0^3} \sqrt{\frac{GM_*}{R_0^3}} \right) \left(\frac{R_0}{r} \right)^3 \nu \sigma. \quad (36)$$

Define a reference temperature T_0 by

$$T_0^4 = \left(\frac{9GM_* M_0}{8 \sigma_B R_0^3} \sqrt{\frac{GM_*}{R_0^3}} \right), \quad (37)$$

we then have

$$T(r) = T_0 \left(\frac{R_0}{r} \right)^{3/4} v^{1/4} \sigma^{1/4}. \quad (38)$$

Finally, from this and equation (28) we obtain the disk half-thickness as

$$\frac{h^2(r)}{R_0^2} = \left(\frac{2k_B T_0 R_0}{GM_* m} \right) \left(\frac{r}{R_0} \right)^{9/4} v^{1/4} \sigma^{1/4}. \quad (39)$$

Inserting $h(r)$ from this equation in the self-consistency equation (25), we obtain an equation relating v to itself and the surface mass density σ :

$$v = \frac{3\lambda^{3/2}}{8\pi^2} \left(\frac{2k_B T_0 R_0}{GM_* m} \right) \left(\frac{r}{R_0} \right)^{3/4} v^{1/4} \sigma^{1/4}, \quad (40)$$

which can be solved to give

$$v = \left(\frac{3\lambda^{3/2}}{8\pi^2} \frac{2k_B T_0 R_0}{GM_* m} \right)^{4/3} \left(\frac{r}{R_0} \right) \sigma^{1/3}. \quad (41)$$

This expression for the effective viscosity is the final outcome of our self-consistency argument. It applies whether or not the disk is in a stationary state.

3. MASS DISTRIBUTION AND SPREADING

3.1. Stationary Mass Flow with Injection at a Given Radius

The mass distribution in the disk evolves according to a diffusion-type equation, which is obtained easily (Pringle 1981) from the height-integrated form of the mass conservation equation

$$\frac{\partial \Sigma}{\partial t} + \frac{1}{r} \frac{\partial}{\partial r} (r \Sigma v) = 0, \quad (42)$$

and combining it with the angular momentum conservation equation (31). Substituting $\partial \Sigma / \partial t$ from equation (42) in equation (31) and assuming a Keplerian velocity profile, i.e., $\Omega^2 = GM_*/r^3$, the angular momentum equation becomes

$$r \Sigma v \frac{\partial}{\partial r} (r^2 \Omega) = \frac{\partial}{\partial r} \left(v_* \Sigma r^3 \frac{\partial \Omega}{\partial r} \right). \quad (43)$$

Equation (43) then gives, for Ω Keplerian, the mass flux as

$$r \Sigma v = -3\sqrt{r} \frac{\partial}{\partial r} (\sqrt{r} v_* \Sigma). \quad (44)$$

When this is used in the mass conservation equation (42), the well-known mass diffusion equation results:

$$\frac{\partial \Sigma}{\partial t} - \frac{3}{r} \frac{\partial}{\partial r} \sqrt{r} \frac{\partial}{\partial r} (\sqrt{r} v_* \Sigma) = 0. \quad (45)$$

This equation disregards the effect of any magnetic torque on the matter. We shall check a posteriori that such a torque is indeed negligible in the solutions we obtain.

Solutions of equation (45) have been found by Pringle (1981) to illustrate matter spreading by the effect of effective viscosity. The viscosity had been taken as constant for simplicity. Here we consider a source term as well and use the self-consistent expression derived in equation (41), which gives quantitatively but not qualitatively different results, still in analytical form. To illustrate specifically how matter distributes itself in a turbulent disk, we set up a solution for an accretion disk that receives matter from a donor at some specific radius $r_0 = x_0 R_0$, as illustrated in Figure 2. In that

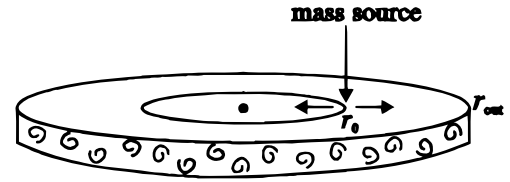


FIG. 2.—A self-consistently turbulent disk receives matter at a hot spot situated at radius r_0 . The turbulent viscosity causes matter to diffuse away from r_0 both inward and outward. At time t , the outer disk radius is $r_{\text{out}}(t)$.

case, equation (45) has an extra source term. We model this source by a Dirac function, which in the axisymmetric model used here means that the source is concentrated on a circle of radius r_0 . In reality, it is known (Horne 1990; Marsh et al. 1990) that the mass enters the disk at a point, the so-called hot spot, not along a circle. However, the Keplerian period being much less than the time for matter to diffuse from the mass injection radius to the accreting star, this does not make any difference for radial motion and radial mass distribution because the matter that enters at the hot spot spreads all around a corresponding circle in the disk in a time short compared to the radial diffusion time. We then expect this simple model to be excellent for this purpose. It is represented by the equation

$$\frac{\partial \Sigma}{\partial t} - \frac{3}{r} \frac{\partial}{\partial r} \sqrt{r} \frac{\partial}{\partial r} (\sqrt{r} v_* \Sigma) = S(t) \delta(r - r_0). \quad (46)$$

A stationary solution to equation (46) exists only if $S(t)$ is independent of time. The injection radius r_0 separates an inner from an outer region, labeled by subscripts “in” and “out.” The total mass flux through a circle of radius r is, from equation (44),

$$\dot{M} = 2\pi r \Sigma v = -6\pi \sqrt{r} \frac{\partial}{\partial r} (\sqrt{r} v_* \Sigma), \quad (47)$$

and the rate of mass injection at r_0 , \dot{M}_0 , is the difference for ϵ approaching zero between $\dot{M}(r_0 + \epsilon)$ and $\dot{M}(r_0 - \epsilon)$. Integrating the source term in equation (46) between $(r_0 - \epsilon)$ and $(r_0 + \epsilon)$, we obtain

$$\dot{M}_0 = 2\pi r_0 S. \quad (48)$$

Similarly, since each gram of injected matter brings with it the specific Keplerian angular momentum at r_0 , $(GM_* r_0)^{1/2}$, the rate of angular momentum injection at r_0 , \dot{J}_0 , is

$$\dot{J}_0 = 2\pi r_0 S \sqrt{GM_* r_0}. \quad (49)$$

In a stationary state, the total fluxes of angular momentum are constant in the inner and outer regions. From equation (31), the total angular momentum flux is

$$\dot{J} = 2\pi r \left(r^2 \Omega \Sigma v - v_* \Sigma r^2 \frac{\partial \Omega}{\partial r} \right). \quad (50)$$

By equation (44), this transforms into

$$\dot{J} = -6\pi r^{5/2} \Omega \frac{\partial}{\partial r} (\sqrt{r} v_* \Sigma) - 2\pi v_* \Sigma r^3 \frac{\partial \Omega}{\partial r}. \quad (51)$$

Let us introduce again the dimensionless quantities v and σ , and the variable

$$x = \frac{r}{R_0}, \quad (52)$$

and associate with R_0 the reference Kepler pulsation

$$\Omega_0 = \sqrt{\frac{GM_*}{R_0^3}}. \quad (53)$$

The form of equation (46) for stationary injection then becomes

$$\frac{\partial \sigma}{\partial \tau} - \frac{1}{x} \frac{\partial}{\partial x} \sqrt{x} \frac{\partial}{\partial x} (x^{3/2} \sigma^{4/3}) = C \delta(x - x_0). \quad (54)$$

The constant C is given in terms of S , itself related to the total mass injection rate (eq. [48]), by

$$C = \frac{SR_0}{3M_0 \sqrt{GM_*/R_0^3}} \left(\frac{3\lambda^{3/2}}{8\pi^2} \frac{2k_B T_0 R_0}{GM_* m} \right)^{-4/3}, \quad (55)$$

and the dimensionless time is

$$\tau = 3 \sqrt{\frac{GM_*}{R_0^3}} \left(\frac{3\lambda^{3/2}}{8\pi^2} \frac{2k_B T_0 R_0}{GM_* m} \right)^{4/3} t. \quad (56)$$

The solution of the stationary form of equation (54) is

$$x^{3/2} \sigma^{4/3} = A \sqrt{x} + B, \quad (57)$$

where A and B are integration constants that take different values $A_{\text{in}}, B_{\text{in}}, A_{\text{out}},$ and B_{out} in the inner and outer regions. Equations (44) and (51) show that the constants A and B are related to the mass and angular momentum accretion rates, respectively. Indeed, from equations (47), (41), (24), and (35), we obtain

$$\dot{M} = -6\pi M_0 \Omega_0 \left(\frac{3\lambda^{3/2}}{8\pi^2} \frac{2k_B T_0 R_0}{GM_* m} \right)^{4/3} \sqrt{x} \frac{\partial}{\partial x} (x^{3/2} \sigma^{4/3}), \quad (58)$$

and from equations (41) and (51) we obtain

$$\begin{aligned} \dot{J} &= 6\pi M_0 \Omega_0^2 R_0^2 \left(\frac{3\lambda^{3/2}}{8\pi^2} \frac{2k_B T_0 R_0}{GM_* m} \right)^{4/3} \\ &\times \left[\frac{1}{2} x^{3/2} \sigma^{4/3} - x \frac{\partial}{\partial x} (x^{3/2} \sigma^{4/3}) \right]. \end{aligned} \quad (59)$$

For the solution (57), this reduces to

$$\dot{M} = -3\pi M_0 \Omega_0 \left(\frac{3\lambda^{3/2}}{8\pi^2} \frac{2k_B T_0 R_0}{GM_* m} \right)^{4/3} A, \quad (60)$$

and

$$\dot{J} = 3\pi M_0 \Omega_0^2 R_0^2 \left(\frac{3\lambda^{3/2}}{8\pi^2} \frac{2k_B T_0 R_0}{GM_* m} \right)^{4/3} B. \quad (61)$$

The mass input at r_0 , \dot{M}_0 , must be balanced by the mass outflow in the disk, away from r_0 :

$$\dot{M}_0 = \dot{M}_{\text{out}} - \dot{M}_{\text{in}}, \quad (62)$$

and the angular momentum input must be similarly balanced:

$$\dot{J}_0 = \dot{J}_{\text{out}} - \dot{J}_{\text{in}}. \quad (63)$$

In equations (62) and (63), the mass and angular momentum fluxes in the disk are defined as positive if oriented outward, while \dot{M}_0 and \dot{J}_0 are positive, since injected mass and angular momentum enter the disk. Equations (62) and (63) relate the integration constants of equation (57) in the inner and outer regions by

$$A_{\text{in}} - A_{\text{out}} = 2Cx_0 = A_0, \quad (64)$$

$$B_{\text{out}} - B_{\text{in}} = 2Cx_0^{3/2}. \quad (65)$$

Since the angular momentum is transported only by matter in this model, it can be shown (Pringle 1981), assuming the boundary layer near the star's surface to be thin, that the inward flux of angular momentum is approximately $\dot{J}_{\text{in}} = \dot{M}_{\text{in}} \Omega_* R_*^2$, so that in fact, defining x_* as the value of the variable x at $r = R_*$:

$$B_{\text{in}} = -A_{\text{in}} \sqrt{x_*}. \quad (66)$$

Then from equation (65),

$$B_{\text{out}} = A_0 \sqrt{x_0} - A_{\text{in}} \sqrt{x_*}, \quad (67)$$

so that the stationary solution (eq. [57]) can be written as

$$x^{3/2} \sigma^{4/3} = A_{\text{in}} (\sqrt{x} - \sqrt{x_*}) \quad x < x_0, \quad (68)$$

$$x^{3/2} \sigma^{4/3} = -(A_0 - A_{\text{in}}) \sqrt{x} + (A_0 \sqrt{x_0} - A_{\text{in}} \sqrt{x_*}) \quad x > x_0. \quad (69)$$

A physically consistent solution should bring matter to the star in the inner region ($\dot{M}_{\text{in}} < 0$, i.e., $A_{\text{in}} > 0$) and away from it in the outer region ($A_0 - A_{\text{in}} > 0$), with an associated outward flux of angular momentum ($A_0 \sqrt{x_0} - A_{\text{in}} \sqrt{x_*} > 0$).

The solution (69) then has outer mass and angular momentum fluxes that, for the solution to be stationary, must be absorbed by a sink at the outer edge of the disk. This outer edge is where the density, as described by equation (69), vanishes. Its normalized radius x_{out} is given by

$$x_{\text{out}} = x_0 \left(\frac{A_0 - A_{\text{in}} \sqrt{x_*/x_0}}{A_0 - A_{\text{in}}} \right)^2. \quad (70)$$

Since x_0 is larger than x_* , and A_{in} is positive, x_{out} is larger than x_0 . The outer matter and angular momentum sink might be identified with the edges of the Roche lobe of the accreting star, where the axisymmetric picture of a flow dominated by the gravitational pull of this star breaks down.

As implied by the localized mass source that appears in it, any solution of equation (54) must exhibit a jump of the derivative with respect to x of $x^{3/2} \sigma^{4/3}$ at x_0 of amplitude $-C(x_0)^{1/2}$. This general condition translates, for the solution (57), into equation (64). The more extended the outer part of the disk, the smaller the derivative of $x^{3/2} \sigma^{4/3}$ on the right-hand side of the injection point, and the smaller the mass flux to this outer region.

3.2. Spreading of Matter Away from the Injection Radius

Alternatively, if one were to insist that the space in which the gravitation of the accreting star dominates is infinite, then there would be no outer sink, and the situation could not be steady until the outer edge of the disk has reached infinity. This happens when $A_{\text{in}} = A_0$. In this case, the injected matter is routed entirely toward the inner part of

the disk, while the outer part has developed into an infinitely extended mass distribution, with density $\sigma_\infty(x)$ given by

$$\sigma_\infty(x) = A_0^{3/4} \frac{(\sqrt{x_0} - \sqrt{x_*})^{3/4}}{x^{9/8}}. \quad (71)$$

The mass of this infinitely extended disk is infinite, since the mass integral diverges when σ scales as $x^{-9/8}$. In this limit, which is reached only when the accretion has been going on for an infinite time, the outer disk has developed into a large mass and angular momentum reservoir.

Since this represents only an asymptotic state, one would rather like to calculate the time evolution of the structure of the disk, which is described by equation (46). Let us then consider this equation again and for a while interpret the reference length R_0 as the total disk radius and the reference mass M_0 as the mass of the disk at time t . Then the dimensionless variables x and σ are, at about that time, of order unity. Equation (46) displays two different characteristic times. The characteristic mass diffusion time is

$$t_{\text{diff}} = \left(\frac{r^2}{3v_*} \right). \quad (72)$$

Associated with mass injection, there is also a characteristic mass-feeding time. As seen in the preceding subsection, only a small part of the total mass injection goes into the outer part of the disk, when the latter has become very extended. Let us call $\dot{M}_{\text{out}}(t)$ the rate of mass feeding to the outer disk at time t . The characteristic time over which the mass of the outer disk evolves is

$$t_{\text{mass}} = \frac{M_{\text{out}}}{\dot{M}_{\text{out}}}. \quad (73)$$

The mass distribution will evolve in the outer disk region in a quasi-static regime if

$$t_{\text{diff}} \ll t_{\text{mass}}. \quad (74)$$

Since the characteristic mass diffusion time depends on the position in the disk, this inequality may be satisfied in certain regions of the disk only, and not in others. To judge the validity of inequality (74), we can estimate M_{out} and \dot{M}_{out} as given by the quasi-static solution (69), neglecting for simplicity the unimportant term $A_{\text{in}}(x_*)^{1/2}$. From equations (35), (52), and (60), we obtain for large x_{out}

$$\begin{aligned} M_{\text{out}} &= 2\pi M_0 \int_{x_0}^{x_{\text{out}}} x \sigma(x) dx \\ &\approx 4\pi M_0 x_0^{5/4} A_0^{3/4} \left(\frac{A_0}{A_0 - A_{\text{in}}} \right)^{5/4} \\ &\quad \times \int_{(A_0 - A_{\text{in}})/A_0}^1 (u - u^2)^{3/4} du, \end{aligned} \quad (75)$$

$$\dot{M}_{\text{out}} = 3\pi\Omega_0 M_0 \left(\frac{3\lambda^{3/2}}{8\pi^2} \frac{2k_B T_0 R_0}{GM_* m} \right)^{4/3} (A_0 - A_{\text{in}}), \quad (76)$$

while from equations (23), (24), and (41), we obtain

$$t_{\text{diff}} = \frac{1}{3\Omega_0} \left(\frac{3\lambda^{3/2}}{8\pi^2} \frac{2k_B T_0 R_0}{GM_* m} \right)^{-4/3} \frac{x}{\sigma^{1/3}(x)}. \quad (77)$$

With these approximations, the inequality $t_{\text{diff}} \ll t_{\text{mass}}$ can be rewritten as

$$\frac{x}{\sigma^{1/3}(x)} \ll \frac{4x_0^{5/4} A_0^{3/4}}{A_0 - A_{\text{in}}} \left(\frac{A_0}{A_0 - A_{\text{in}}} \right)^{5/4} \int_0^1 (u - u^2)^{3/4} du. \quad (78)$$

Since x and σ are of order unity, we see that, when the outer disk expands and A_{in} becomes closer to A_0 , the right-hand side of this inequality overwhelms the left-hand side. As a result, the quasi-static approximation becomes asymptotically more and more valid.

It is then easy to calculate the motion of the outer edge of the disk. The quasi-static approximation allows us to calculate the mass stored at time t in the outer part of the disk, which, from equations (35) and (52), can be written as

$$M_{\text{out}}(t) = M_0 \int_{x_0}^{x_{\text{out}}} 2\pi x \sigma(x) dx. \quad (79)$$

Let us recall that σ is a function of time also, since the parameter A_{in} that enters in expression (69) changes with time. Equations (58) and (64) give the rate of mass injection in the expanding outer part of the disk as

$$\dot{M}_{\text{out}} = 3\pi M_0 \Omega_0 \left(\frac{3\lambda^{3/2}}{8\pi^2} \frac{2k_B T_0 R_0}{GM_* m} \right)^{4/3} (A_0 - A_{\text{in}}). \quad (80)$$

Another independent equation for \dot{M}_{out} can be obtained by inserting the expression (69) for σ in the expression (79) for M_{out} above and differentiating the result with respect to time, noting that x_{out} and A_{in} both depend on it. This gives after a little algebra

$$\begin{aligned} \frac{\dot{M}_{\text{out}}}{M_0} &= \frac{dA_{\text{in}}}{dt} \\ &\quad \times \int_{x_0}^{x_{\text{out}}} \frac{2\pi x (\sqrt{x} - \sqrt{x_*}) dx}{x^{9/8} [(A_0 \sqrt{x_0} - A_{\text{in}} \sqrt{x_*}) - (A_0 - A_{\text{in}}) \sqrt{x}]^{1/4}}. \end{aligned} \quad (81)$$

Equating these two expressions of \dot{M}_{out} , we obtain an equation that describes the time-evolution of $(A_0 - A_{\text{in}})$, namely,

$$\begin{aligned} \frac{d(A_0 - A_{\text{in}})}{dt} &\left[\int_{x_0}^{x_{\text{out}}} \frac{2\pi x (\sqrt{x} - \sqrt{x_*}) dx}{x^{9/8} (\sqrt{x_{\text{out}}} - \sqrt{x})^{1/4}} \right] \\ &= -3\pi\Omega_0 \left(\frac{3\lambda^{3/2}}{8\pi^2} \frac{2k_B T_0 R_0}{GM_* m} \right)^{4/3} (A_0 - A_{\text{in}})^{5/4}. \end{aligned} \quad (82)$$

The integral over x on the left-hand side is not simple, which makes it difficult to express and solve this differential equation in the most general case. Asymptotically, however, the outer radius grows much larger than the injection radius and the inner disk radius, so that the integral can be calculated easily, with the result that

$$\begin{aligned} &\left[\int_{x_0}^{x_{\text{out}}} \frac{2\pi x (\sqrt{x} - \sqrt{x_*}) dx}{x^{9/8} (\sqrt{x_{\text{out}}} - \sqrt{x})^{1/4}} \right] \\ &\approx 2\pi x_{\text{out}}^{9/8} \int_0^1 u^{3/2} (1 - \sqrt{u})^{-1/4} du. \end{aligned} \quad (83)$$

The value of the integral from 0 to 1 on the right-hand side is 3/4. Inserting this result and the expression given by equation (70) for x_{out} in the equation (82) for $(A_0 - A_{\text{in}})$ gives

$$\frac{d}{dt} (A_0 - A_{\text{in}})^{-5/2} = \frac{4}{5} \Omega_0 \left(\frac{3\lambda^{3/2}}{8\pi^2} \frac{2k_B T_0 R_0}{GM_* m} \right)^{4/3} x_0^{-9/8} A_0^{-9/4}. \quad (84)$$

From this equation we obtain $(A_0 - A_{in})$, which is found to decrease with time as $t^{-2/5}$, and finally, still neglecting x_* , an expression for the asymptotic growth of the outer disk radius:

$$x_{out} = (\Omega_0 t)^{4/5} x_0 A_0^2 \left[4 \left(\frac{3\lambda^{3/2}}{8\pi^2} \frac{2k_B T_0 R_0}{GM_* m} \right)^{4/3} \right]^{4/5} \times (5x_0^{9/8} A_0^{9/4})^{-4/5}. \quad (85)$$

The disk radius is then seen to expand as $t^{4/5}$ asymptotically, with less and less of the accreted mass gathering in the outer part, and more and more being routed toward the star.

4. MAGNETIC FIELD DIFFUSION

4.1. Field Diffusion in a Slim Disk

Now we want to investigate the evolution of magnetic fields threading the turbulent disk to understand, in particular, the diffusion of matter through it. The turbulence causes diffusion of that part of the magnetic field that is organized on the large scale. In this section only these large-scale fields are considered explicitly. The effect of small-scale fields is represented by the turbulent transport coefficients. We ignore, for simplicity essentially, any dynamo effect. Dynamo-generated fields in thin accretion disks are likely to be on a scale not much larger than the thickness of the disk (Pudritz 1981; Stepinsky & Levy 1989) and could possibly give rise to a similarly small-scale component in the disk's corona, although this question deserves further study because the dynamics of these structures in the corona has not yet been investigated in detail. The field evolution equation inside the disk is then

$$\frac{\partial \mathbf{B}}{\partial t} = \nabla \times (\mathbf{v} \times \mathbf{B}) - \nabla \times [\eta_* (\nabla \times \mathbf{B})], \quad (86)$$

where η_* is the turbulent magnetic diffusivity, which scales as v_* (eqs. [41], [23], [24], and [35]), unless some process unrelated to MHD turbulence, for example ambipolar diffusion, gives rise to a magnetic diffusivity much in excess of v_* . Here we assume this not to be so. The magnetic Prandtl number for turbulent transport coefficients, η_*/v_* , should be of the order of unity, but not necessarily exactly equal to it. Pouquet, Frisch, & Léorat (1976) find it equal to 5/7 in their model. Therefore, we write

$$\eta_* = v_{*0} \eta = p_t v_{*0} v. \quad (87)$$

Because of axisymmetry, the poloidal magnetic field can be expressed in terms of a toroidal vector potential that can be written conveniently as

$$\mathbf{B}_P = \nabla \times \left[\frac{A(r, z)}{r} \mathbf{e}_\theta \right]. \quad (88)$$

We call the function A the flux function, since it is proportional to the flux through a circle centred on the axis and stretching out to the point (r, z) . The components of \mathbf{B} are

$$B_r = -\frac{1}{r} \frac{\partial A}{\partial z}, \quad B_z = +\frac{1}{r} \frac{\partial A}{\partial r}, \quad B_\theta = B_\theta(r, z). \quad (89)$$

Magnetic surfaces, generated by the rotation of field lines about the axis, are surfaces of constant $A(r, z)$. The velocity field is represented by its components

$$\mathbf{v} = v(r, z)\mathbf{e}_r + r\Omega(r)\mathbf{e}_\theta + v_z\mathbf{e}_z. \quad (90)$$

Some algebra shows that the poloidal components of equation (86) can be gathered in the following equation:

$$\nabla \left[\frac{\partial A}{\partial t} + (\mathbf{v} \cdot \nabla)A - \eta_* \left(\frac{\partial^2 A}{\partial z^2} + r \frac{\partial}{\partial r} \frac{1}{r} \frac{\partial A}{\partial r} \right) \right] = 0, \quad (91)$$

which integrates to

$$\frac{\partial A}{\partial t} + (\mathbf{v} \cdot \nabla)A - \eta_* \left(\frac{\partial^2 A}{\partial z^2} + r \frac{\partial}{\partial r} \frac{1}{r} \frac{\partial A}{\partial r} \right) = \Lambda(t). \quad (92)$$

The space-independent function $\Lambda(t)$ can be taken to be zero because it can be transformed away by the gauge transformation

$$\hat{A} = A + \int_0^t \Lambda(t') dt'. \quad (93)$$

The equation that describes the evolution of the flux function is then

$$\frac{\partial A}{\partial t} + v_r \frac{\partial A}{\partial r} + v_z \frac{\partial A}{\partial z} - \eta_* \left(\frac{\partial^2 A}{\partial z^2} + r \frac{\partial}{\partial r} \frac{1}{r} \frac{\partial A}{\partial r} \right) = 0. \quad (94)$$

Since the disk is thin, all the terms in this equation are not of comparable order of magnitude. The radial gradient scale should be of order r , while the vertical one should not be much smaller than the disk thickness $h(r)$, but might be much larger. The horizontal and vertical fluid velocity are related by the mass conservation equation, which in a stationary state and for moderate compressibility implies that

$$\frac{v_r}{r} \approx \frac{v_z}{h}, \quad (95)$$

while the diffusivity v_* is of the order of the Shakura-Sunyaev value, in agreement with our own result (eq. [12]),

$$v_* \approx \eta_* \approx \Omega h^2. \quad (96)$$

An estimate of the radial velocity v_r results from the angular momentum equation (43),

$$v_r \approx \frac{v_*}{r} \approx \frac{\Omega h^2}{r}. \quad (97)$$

To compare terms in equation (94), we need an order-of-magnitude estimate of $(\partial A/\partial r)$ and $(\partial A/\partial z)$. Obviously

$$\frac{\partial A}{\partial r} \approx \frac{A}{r}, \quad (98)$$

but $\partial A/\partial z$ cannot be of order A/h because by equation (89) the component B_r would be much larger than B_z . If such an estimate were to be correct, the first diffusive term on the right-hand side of equation (94) would be of order $\eta_* A/h^2 \approx \Omega h$, much larger than all the other terms. As a result, in a time no longer than the Keplerian period, $\partial^2 A/\partial z^2$ would relax to much smaller values, until it becomes comparable to at least one of the other space derivative terms. Straightforward estimates give

$$v_r \frac{\partial A}{\partial r} \approx A \Omega \frac{h^2}{r^2}, \quad \eta_* r \frac{\partial}{\partial r} \frac{1}{r} \frac{\partial A}{\partial r} \approx A \Omega \frac{h^2}{r^2}. \quad (99)$$

Let l_z be the gradient scale for A in the vertical direction. Then

$$v_z \frac{\partial A}{\partial z} \approx A \Omega \frac{h^2}{r^2} \frac{h}{l_z}, \quad \eta_* \frac{\partial^2 A}{\partial z^2} \approx A \Omega \frac{h^2}{l_z^2}. \quad (100)$$

Since l_z must be much larger than h , as discussed above, the term $v_z \partial A / \partial z$ is always negligible as compared to the other terms in equation (99), and the second z -derivative term can be challenged by them only if l_z is of order r or larger.

Thus, $A(r, z)$ can be very well approximated inside the disk at fixed r by a parabolic function of z , and A does not change very much over a disk thickness. So we can write approximately

$$A(r, z) = A(r, 0) + \frac{z^2}{2} A_2, \quad (101)$$

where A_2 is the value of $\partial^2 A / \partial z^2$ calculated at the center plane of the disk at distance r from the center. Equation (101) gives for the first-order derivative

$$\frac{\partial A}{\partial z} = A_2(r), \quad (102)$$

and the value of this quantity at the upper disk surface is approximately

$$\left(\frac{\partial A}{\partial z} \right)_+ = h(r) A_2(r). \quad (103)$$

The second derivative, almost uniform in this approximation, can be expressed in terms of this upper surface value by

$$A_2 = \left(\frac{\partial^2 A}{\partial z^2} \right)(r, 0) \approx \frac{1}{h(r)} \left(\frac{\partial A}{\partial z} \right)_+. \quad (104)$$

Considering equation (104) and neglecting as suggested the vertical advection term, equation (94) reduces to

$$\frac{\partial A}{\partial t} + v_r \frac{\partial A}{\partial r} - \eta_* \left[\frac{1}{h} \left(\frac{\partial A}{\partial z} \right)_+ + r \frac{\partial}{\partial r} \frac{1}{r} \frac{\partial A}{\partial r} \right] = 0, \quad (105)$$

where $v_r(r)$ and $h(r)$ are to be taken from the hydrodynamical solution, and the upper surface derivative $(\partial A / \partial z)_+$ results from the structure of the magnetic field in the region exterior to the disk. This region, in which equation (94) does not apply because the coronal medium is not regarded as dissipative, should be examined separately, which we do later on.

4.2. Flux Diffusion in a Thin Disk Connected to an Open Magnetic Structure

To be specific, let us assume that the magnetic field that threads the disk has, in the outer medium, an open structure. The situation in which it is connected to a central object is different and is dealt with in Bardou & Heyvaerts (1996). The outer medium is assumed to consist of a nondissipative plasma, an assumption that could require reconsideration because of possible turbulence in this region also. The rotation of the disk generates in this outer medium an azimuthal field component. It is conceivable that a wind could be blown as a result of this interaction under certain conditions (Blandford & Payne 1982; Ferreira & Pelletier 1993a), even if the disk plasma is cold. Describing it

roughly, the process that imposes rotation in the outer medium by tethering to the disk through the magnetic field is similar to the emission of a torsional Alfvén wave from the disk in the outer medium, though possibly a nonlinear one. The twist of the field in the outer medium would then be approximately one turn per Alfvén travel length in one rotation period. We expect

$$\frac{B_\theta}{B_z} \approx \frac{r \Omega(r)}{v_{\text{Aext}}}. \quad (106)$$

If the outer medium is very tenuous, this ratio is very small, and we can treat the external field as potential. For complete consistency, the density of the external medium should be calculated from a modeling of the external zone incorporating the heating and evaporation mechanisms that could affect the disk–outer medium interaction, and taking into account the possibility of a wind blowing off the disk.

When the external field is indeed potential, the currents that create it are located at infinity or in the disk. The currents at infinity create a permanent field, not affected by flows in the disk, which we refer to as the external field. The currents in the disk have a structure similar to surface currents, since the disk is thin. Their azimuthal surface current density, i_θ , is supported by a jump in the radial component of the field between the upper and lower disk surface. Assuming a symmetry between upper and lower hemispheres such that the vertical field components have the same sign but the radial ones have opposite signs at symmetric point, we find from Ampère's law

$$\mu_0 i_\theta = 2B_{r+}, \quad (107)$$

where B_{r+} is the radial component of the field at the upper disk surface

$$B_{r+}(r) = B_r[r, h(r)] = -\frac{1}{r} \left(\frac{\partial A}{\partial z} \right)_+. \quad (108)$$

The flux function in the medium exterior to the disk can then be separated into a part produced by currents at infinity A_0 and a part produced by disk currents a :

$$A(r, z) = A_0(r, z) + a(r, z). \quad (109)$$

The function $a(r, z)$ is the unknown of this problem. Since the field is potential, a can be calculated from its value on the disk, at $z = 0$. So the ultimate unknown is the function $a(r, 0)$. Solving a potential problem to express $a(r, z)$ in terms of $a(r, 0)$ will eventually provide an expression of a Poisson integral form for the upper disk surface derivative $(\partial a / \partial z)_+$ in terms of $a(r, 0)$. Substituting this expression in equation (105), we shall obtain an integro-differential equation for the one-dimensional function $a(r, 0)$. The effect of the variation with z of $a(r, z)$ in the disk will then have been integrated in terms of $a(r, 0)$ alone, the memory of this vertical structure surviving by the presence of the disk thickness $h(r)$ in equation (105) and in the final equation that we will now derive.

The flux function $A(r, z)$ is related to the components of the magnetic field by equations (89). From Ampère's equation, we find that it satisfies the Poisson-like equation

$$DA = -\mu_0 j_\theta, \quad (110)$$

where D is an elliptic operator that differs slightly from the cylindrical Laplacian because $A(r, z)$ is not exactly a com-

ponent of the vector potential

$$D = \frac{\partial}{\partial r} \frac{1}{r} \frac{\partial}{\partial r} + \frac{\partial}{\partial z} \frac{1}{r} \frac{\partial}{\partial z}. \quad (111)$$

In the region outside the disk, in which the field is potential, the source term in equation (110) vanishes, and the function $a(r, z)$ is in this region the solution of

$$Da = 0. \quad (112)$$

The solution of equation (112) can be obtained in terms of boundary values of a by an appropriate Poisson formula, which can be obtained from the Green's function of equation (110) with homogeneous boundary conditions (i.e., a function vanishing on the boundary and at infinity). Let $G(r, z | r', z')$ be that function, responding to a localized source at r', z' . It is the solution of

$$DG = \delta(r - r')\delta(z - z'). \quad (113)$$

In the present problem, the domain Q of calculation is the quarter-plane in which r and z are both positive. Its boundary Γ consists of positive r - and z -axes. The Poisson formula is deduced from the Green's function in a standard way, as described in the book by Courant & Hilbert (1937). It is only necessary that the operator D obeys a Green's formula that ensures that for any pair of functions u and v ,

$$\iint_Q (uDv - vDu) dr dz = \int_\Gamma \left(\frac{u}{r} \mathbf{n}_{\text{out}} \cdot \nabla v - \frac{v}{r} \mathbf{n}_{\text{out}} \cdot \nabla u \right) ds, \quad (114)$$

where \mathbf{n}_{out} is the outgoing normal to the domain Q and the sense of integration on the boundary is defined by the usual convention that the inside of the domain is on the left. The validity of equation (114) in the present case can be proved directly by integration by parts. If then g is the value of the function a on the boundary, the solution of equation (112) is

$$a(r, z) = \int_\Gamma \frac{g}{r} (\mathbf{n}_{\text{out}} \cdot \nabla G) ds. \quad (115)$$

In the present particular case, this gives explicitly, since g vanishes on the polar axis,

$$a(r, z) = - \int_0^\infty dx \frac{a(x, 0)}{x} G_y(r, z | x, 0), \quad (116)$$

where G_y denotes the partial derivative of the Green's function $G(r, z | x, y)$ with respect to the last variable y .

The Green's function is easily calculated explicitly by noting that G as defined by equation (113) is the flux function produced by a current ring of intensity $(-\mu_0)$ and radius r' at altitude z' . The flux function must vanish on the boundary Γ , a condition that can be taken care of by the method of images. Using the Biot-Savart law to calculate the flux function of a current ring (Jackson 1975), we obtain

$$G(r, z | x, y) = \frac{rx F(k_+)}{\pi \sqrt{(r+x)^2 + (z+y)^2}} - \frac{rx F(k_-)}{\pi \sqrt{(r+x)^2 + (z-y)^2}}, \quad (117)$$

where the variables k_+ and k_- are defined by

$$k_+^2 = \frac{4rx}{(r+x)^2 + (z+y)^2}, \quad k_-^2 = \frac{4rx}{(r+x)^2 + (z-y)^2}, \quad (118)$$

and the function $F(k)$ is defined in terms of the complete elliptic integrals $E(k)$ and $K(k)$ by

$$F(k) = \frac{2-k^2}{k^2} K(k) - \frac{2}{k^2} E(k). \quad (119)$$

The function $F(k)$ has an integral representation

$$F(k) = \int_0^{\pi/2} \frac{(2 \sin^2 x - 1)}{\sqrt{1 - k^2 \sin^2 x}} dx. \quad (120)$$

Using these results to make the solution obtained in equation (116) explicit, we finally obtain

$$a(r, z) = \int_0^\infty dx \frac{1}{2\pi} \frac{a(x, 0)}{x} \frac{z}{\sqrt{(r+x)^2 + z^2}} \times [k^2 F(k) + k^3 F'(k)], \quad (121)$$

where now

$$k^2 = \frac{4rx}{(r+x)^2 + z^2}. \quad (122)$$

When z approaches zero, the factor of $a(x, 0)$ in equation (121) approaches a Dirac function, as it should. Indeed, some algebra shows that in this limit, equation (121) becomes approximately

$$a(r, z) = \int_0^\infty dx a(x, 0) \left[\frac{1}{\pi} \frac{z}{(r-x)^2 + z^2} \right]. \quad (123)$$

Equation (123) is sufficient to calculate $\partial a / \partial z$ on the boundary. We find for small z

$$\frac{\partial a}{\partial z}(r, z) = \int_0^\infty dx a(x, 0) \frac{(r-x)^2 - z^2}{\pi [(r-x)^2 + z^2]^2}. \quad (124)$$

The rational fraction on the right-hand side of equation (124) is an even function of $(r-x)$ that acquires for small z a deep negative spike at $x=r$ of width $2z$ and depth $-1/(\pi z^2)$. The integral that appears in equation (124) is convergent, even when $a(x, 0)$ does not vanish at infinity. Let us convert it into

$$\begin{aligned} \frac{\partial a}{\partial z}(r, z) = & \int_0^\infty dx [a(x, 0) - a(r, 0)] \frac{(r-x)^2 - z^2}{\pi [(r-x)^2 + z^2]^2} \\ & + a(r, 0) \int_0^\infty dx \frac{(r-x)^2 - z^2}{\pi [(r-x)^2 + z^2]^2}. \end{aligned} \quad (125)$$

The first integral approaches a principal part distribution when z approaches zero. Indeed, in the vicinity of r , one can separate, for small z , a symmetric interval, $(r-\epsilon, r+\epsilon)$, much larger than z , but much less than the characteristic gradient scale of $a(x, 0)$, such that $[a(x, 0) - a(r, 0)]$ can be approached by its first-order Taylor expansion. The integral is then zero by parity on this interval. Outside this interval, z can be neglected. As $z \rightarrow 0$, the integral then approaches a principal part. The second integral can be evaluated explicitly. This finally gives, for vanishingly small z ,

$$\left(\frac{\partial a}{\partial z} \right)_+ = P \int_0^\infty dx \frac{[a(x, 0) - a(r, 0)]}{\pi [(r-x)^2]} - \frac{a(r, 0)}{\pi r}, \quad (126)$$

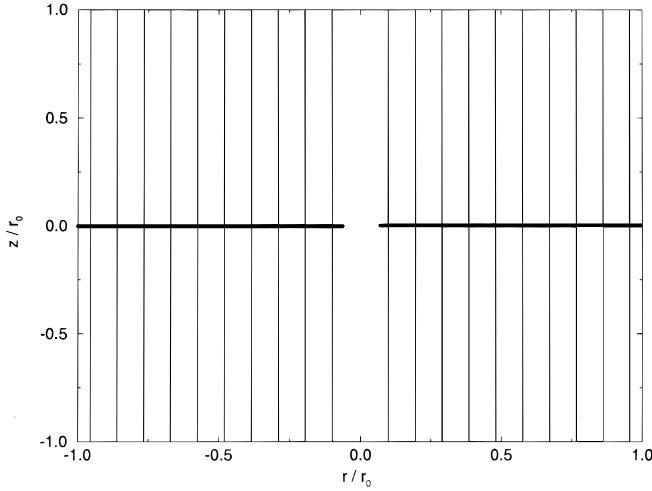


FIG. 3a

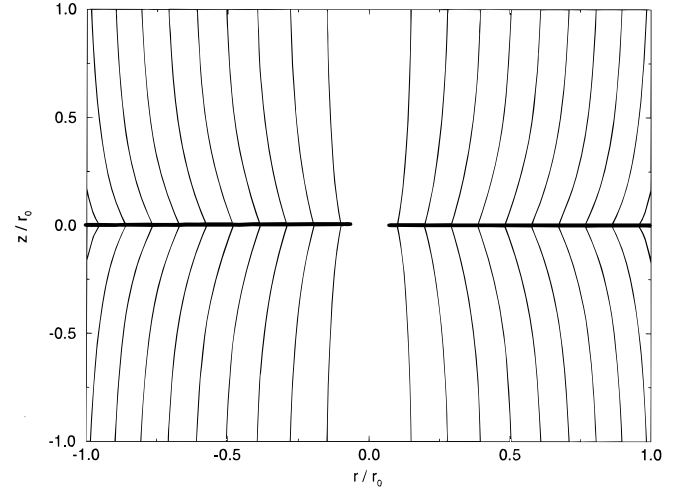


FIG. 3b

FIG. 3.—The field line geometry for a uniform magnetic field suffering dragging and diffusion from an accretion disk in a turbulence regime driven by magnetic shearing instability, or, more generally, by any turbulence having an injection scale comparable to the disk thickness. This geometry has been calculated here according to eq. (132), matter being injected at $r_0 = 10^{10}$ cm, with an accretion rate $\dot{M}_0 = 10^{-8} M_\odot \text{ yr}^{-1}$. The magnetic Prandtl number P is (a) $5/7$ and (b) 0.1 .

where P denotes the principal part. To be specific, let us consider that the external field is a uniform one, with flux function $A_0(r, z) = B_0 r^2/2$. Then the field evolution equation (105) can be written for the unknown function a as

$$\frac{\partial a}{\partial t} + rB_0 v + v \frac{\partial a}{\partial r} = \eta_* r \frac{\partial}{\partial r} \frac{1}{r} \frac{\partial a}{\partial r} + \frac{\eta_*}{h} P \int_0^\infty dx \frac{[a(x, 0) - a(r, 0)]}{\pi[(r-x)^2]} - \frac{\eta_*}{h} \frac{a(r, 0)}{\pi r}. \quad (127)$$

Again, the disk thickness $h(r, t)$, the radial velocity $v(r, t)$, and the turbulent resistivity $\eta_*(r, t)$ are to be taken from the hydrodynamical solution sketched before. Equation (127) is an improved form of a similar equation derived by Lubow et al. (1994).

4.3. Thin Disks Supported by Magnetic Shearing Turbulence are Low Magnetic Reynolds Number Systems

An important aspect of the disks we have just discussed is that they are low effective magnetic Reynolds number systems. To see this, let us compare in equation (127) the advection term $v \partial a / \partial r$ with the resistive terms. The dominant ones, namely, the second and third ones on the right, are of order $(\eta_* a)/(rh)$. Note that it has been necessary to carry out the calculation in § 4.2 to make sure of this, the order of magnitude of these terms being smaller than the incorrect estimate $(\eta_* a)/h^2$ that would have resulted from estimating $\partial^2 a / \partial z^2$ as being of order a/h^2 . The first term on the right of equation (127) is of order $(\eta_* a)/r^2$ and is much smaller than the two following ones. Since η_* is of order Ωh^2 and the radial velocity v is of order $\Omega h^2/r$ (eq. [97]), we estimate the effective magnetic Reynolds number of the disk R_m to be

$$R_m = \frac{v \partial a / \partial r}{\eta_* a / hr} \approx \frac{h}{r}. \quad (128)$$

This shows that the advection of the field self-created by the disk is much smaller than its diffusion, a characteristic of a low magnetic Reynolds number system. This is to be com-

pared to the Reynolds number R_v associated with the effective viscosity, which from equation (97) can be estimated as being of order

$$R_v = \frac{vr}{\nu_*} \approx 1. \quad (129)$$

The magnetic Reynolds number is much smaller because the vertical gradient plays a role in the resistive diffusion of magnetic fields, which it does not do in the viscous diffusion of matter. As a result of these estimates, we find that the field diffusion equation (127) reduces to

$$\frac{\partial a}{\partial t} + vrB_0 = \frac{\eta_*}{h} P \int_0^\infty dx \frac{[a(x, 0) - a(r, 0)]}{\pi[(r-x)^2]} - \frac{\eta_*}{h} \frac{a(r, 0)}{\pi r}. \quad (130)$$

This equation describes the resistive evolution of a magnetic field associated with a disk current generated by the electromotive field vB_0 that results from the external field and the radial velocity. In the present approximation, in which the reaction of Lorentz forces on the plasma motion is neglected, the latter is the result of a purely hydrodynamical calculation. This means that the disk behaves in this limit just as any laboratory dynamo: an electromotive force is developed from its imposed motion in an externally imposed field, which generates resistively an electric current. This becomes very clear if we consider a stationary state. Note that, by equations (126) and (108), the right side of equation (130) is simply $(-r\eta_* B_r +)/h$. Defining an effective turbulent electrical conductivity s_* by $s_* = 1/(\mu_0 \eta_*)$ and using equation (107), equation (130) can be reduced to the simple form of Ohm's law,

$$i_\theta = 2hs_*(-vB_0). \quad (131)$$

Here $(-vB_0)$ is the θ -component of the electromotive force $\mathbf{v} \times \mathbf{B}_0$, and $i_\theta/(2h)$ is the θ -component of the volume- (as opposed to surface-) electric current density j_θ . Equation (131) is simply the azimuthal component of the familiar Ohm's equation $\mathbf{j} = s_*(\mathbf{v} \times \mathbf{B}_0)$. Since the current i_θ that generates the magnetic field perturbation is obtained from

equation (131), the associated magnetic field can be calculated simply from Biot and Savart's law with this known source. This gives

$$a(r, z) = - \int_0^\infty dr' \left[\frac{2B_0 h(r') v_r(r')}{\pi \eta_*(r')} \right] \frac{rr'}{\sqrt{(r+r')^2 + z^2}} F(k), \quad (132)$$

where k is the variable defined in equation (122).

We have, for illustration, calculated this magnetic field for the flow pattern calculated in § 3a. The results are presented in Figure 3, where we have taken the magnetic Prandtl number to be equal to 5/7, as suggested from the work by Pouquet et al. (1976). It is seen that the external field suffers completely negligible distortion by the advective radial flow. The angle of the magnetic field with the vertical is similarly exceedingly small. The general results of our calculations agree with those of Lubow et al. (1994). A smaller Prandtl number would give rise to a stronger distortion of the magnetic field, as seen in Figure 3b, which has been calculated for a Prandtl number equal to 1/10. We do not regard, however, Prandtl numbers that differ substantially from unity as realistic when both viscosity and magnetic diffusivity originate from the turbulence. We could envisage the magnetic Prandtl number to differ strongly from unity when the ambipolar diffusion is more effective in letting matter slip through the field than the turbulent magnetic diffusivity itself. But this would correspond to Prandtl numbers larger, not smaller, than unity, and the distortion of the field lines would be even smaller than calculated here. Alternatively, the Prandtl number could be strongly affected if the turbulent motion were predominantly in the disk plane rather than three-dimensional. This could occur if the external field were very strong. Another point worth stressing is that the ratio $h(r)v_r(r)/\eta_*(r)$ is found to be independent of the parameter λ defined in equation (4). This is because the radial drift timescale is the viscous timescale, so that $rv_r(r)/v_*(r)$ is necessarily independent of λ , as is h/r . So our results are not sensitive to the precise way in which the connection between the turbulence spectrum and the effective viscosity is modeled.

5. CONCLUSIONS

The small angle between the field and the vertical to the disk has the important consequence that a cold centrifugally driven MHD wind cannot be launched from such a disk. Indeed, Blandford & Payne (1982) have shown that a minimum angle of 30° between the field and the disk normal is necessary for a wind to be blown merely by the centrifugal effect, without the assistance of pressure. Hence, our neglect of angular momentum loss by an MHD wind in evaluating the radial velocity in our purely viscosity-driven inflow model of § 3 has been a self-consistent assumption. Indeed, since no wind is blown in the environment of the disk, the external field is not loaded with plasma, and so there is no field twist and consequently no radial surface current component that could exert a torque of magnetic origin on the disk. We conclude that an accretion disk supported by an effective viscosity due to magnetic-shearing turbulence is a low magnetic Reynolds number system, which accretes because of angular momentum diffusion due to effective viscosity and cannot blow any cold centrifugally driven MHD wind.

Our conclusions agree on this point with those of Ferreira & Pelletier (1995), who have discussed in which parameter regime a consistent disk-wind system, in which accretion is dominantly driven by angular momentum loss to a wind, could exist. They found this to be possible only if the effective resistivity and the magnetization parameter are such that the vertical scale of variation of the flux function is much larger than the disk thickness, but not too much larger, i.e., field lines have to emerge from the disk not too perpendicular to the disk plane. They find that the most viable magnetic configuration for MHD wind-driven accretion is when this scale is of order $[rh(r)]^{1/2}$. Here this length, which is defined as $[(\partial^2 A / \partial z^2) / A]^{-1/2}$, is seen from equations (104), (109), and (126) to be in fact larger by a factor $(A_0/a)^{1/2}$, which is a very large number. Our conclusions also agree with the results of Lubow et al. (1994) and the more recent study by Agapitou & Papaloizou (1995), who have also found that when the magnetic Prandtl number of the turbulence η_*/v_* is not small, and the effective viscosity of order of the Shakura-Sunyaev value, a thin disk is a low magnetic Reynolds number system. These authors did not calculate the actual value of effective viscosity and magnetic diffusivity, but they stressed the fact that when the magnetic Prandtl number of the turbulence is, as expected, of order unity, flux diffusion should be so effective that the Blandford-Payne criterion for blowing cold centrifugally driven winds would not be satisfied at all, a conclusion that is entirely supported by our own results. The numerical illustration of the results of Lubow et al. (1994) has been made, however, for magnetic Prandtl numbers that are, in our view, unrealistically small, and that tend to hide the fact that magnetic diffusivity is so effective.

We do not mean, though, that all accretion disks are unable to launch cold centrifugally driven MHD winds. Our conclusion applies only to those disks that are able to develop turbulence having eddies as large as the disk thickness itself. In this case, our analysis shows that a disk in which accretion is supported by effective viscosity, no cold wind being centrifuged away, is a consistent solution. It may not be the unique solution, though. On the one hand, a thermally driven wind could still be emitted by the disk. We do not explore this possibility further because it calls for a theory of the heating of the coronal region just above the disk. On the other hand, it is a priori conceivable also that solutions other than the one we have just described exist for the same model parameters (magnetic field at infinity, mass of the accreting star, accretion rate), in which a faster accretion velocity, allowing for a much larger value of B_{r+}/B_z , would be supported by angular momentum loss to a cold wind. We believe, though, that this is somewhat unlikely because the effective Reynolds number in the regime we have calculated is so small that the accretion velocity would have to grow enormously larger in a wind-driven regime to compensate. Ferreira & Pelletier (1993a, 1993b, 1995) have shown that self-consistent stationary accretion-ejection structures must be rather fine-tuned systems. Conditions for such structures to exist are, according to Ferreira & Pelletier (1995), that the effective viscosity scale as $\alpha_m v_A h$, i.e., be proportional to the product of the Alfvén velocity associated with the global field and the disk thickness, and that the magnetization parameter $\mu = v_A^2 / \Omega^2 h^2$, which is of the order of the inverse of the parameter beta of the plasma of the disk, be of order unity. Another major constraint is that their parameter Γ , which is proportional to $3/\alpha_m^2$, be of

order unity, a condition that expresses the requirement that the forces that propel the wind act near the surface of the accretion disk. Altogether, these parameters must be such that the three field components at the disk's surface are comparable. It is conceivable that such conditions could result naturally, as claimed by these authors, from the saturation of MHD instabilities. Further studies are necessary to settle this issue. We note, however, that the condition deduced by Ferreira & Pelletier (1995) concerning the magnetization parameter in wind-driven accretion disks is necessarily violated when the turbulence results from the magnetic shearing instability. As discussed in § 2.6, this instability occurs only in high-beta systems. It is quenched when β approaches unity. It is interesting to note that the magnetic shearing instability taps the free energy of differential rotation. In some sense, as stressed also by Brandenburg et al. (1995), the initial weak field is but a catalyst that allows the instability to proceed, but the turbulence level eventually reached is only very weakly related to the initial amplitude of this field.

Our conclusions are illustrated in Figure 4. As discussed at the end of § 2.6, different effective viscosity regimes are to be expected if the field threading the disk is large enough to

quench the magnetic shearing instability. Disks of objects that have a magnetopause at the disk's inner edge necessarily have an inner zone that is not subject to this instability. It is conceivable, but not yet proved, that such disks would accrete by emission of an MHD wind from their innermost regions, as also suggested by Lubow & Spruit (1995). This, according to Ferreira & Pelletier (1995), implies, for stationary state, that in some inner disk region, the turbulence would not be due to a hydrodynamically driven instability, but would instead involve an MHD instability, with a characteristic scale shorter than the disk thickness (otherwise the magnetic Reynolds number would still be too small), saturating at a level that effectively depends on the initial magnetic field value.

Note finally that the field line structure outside the disk should differ significantly if the external field is that of the accreting star, and not that of remote sources. The study of what happens in this case is treated in the paper by Bardou & Heyvaerts (1996).

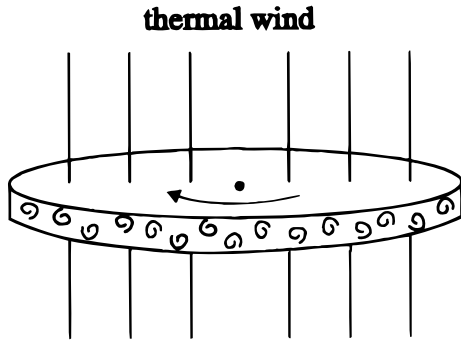


FIG. 4a

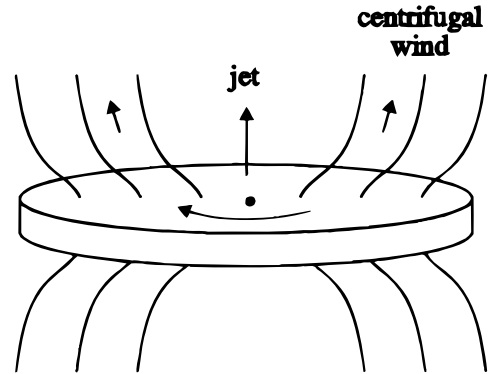


FIG. 4b

FIG. 4.—A schematic representation of the magnetic structure around a disk interacting with a uniform potential field. (a) The injection scale of the turbulence is in this case comparable to the disk thickness. The disk is then a low magnetic Reynolds number system, and the magnetic field produced by electric currents flowing in the disk is negligible. No centrifugally driven cold wind can be blown from such a disk. If a wind is emitted, it must be thermally driven. (b) The injection scale of the turbulence is in this case much smaller than the disk thickness. The magnetic Reynolds number is larger than in (a), and the magnetic field produced by currents flowing in the disk is not negligible to the potential field. A cold centrifugally driven wind could be emitted from such a disk and control the angular momentum loss of accreted matter. A completely laminar situation may be impossible because a consistent stationary solution for the disk-wind connection requires some dissipation (Ferreira & Pelletier 1995).

APPENDIX

The spectrum (14) gives rise to the following rms velocity $\langle v^2 \rangle^{1/2}$:

$$\langle v^2 \rangle = \int d^3k W(k) = 6\pi q C(q) \epsilon^{2/3} k_{\text{inj}}^{-2/3}. \quad (133)$$

We have used the fact that the volume element in the modified wavevector space K is related to that in real wavevector space by

$$dk_r dk_\theta dk_z = q dK_r dK_\theta dK_z. \quad (134)$$

The turbulence is anisotropic, and in this particular case its correlation length in the θ -direction is much larger than in the poloidal directions. Since we are interested in transport properties in the radial direction, it is the correlation length in the meridional plane that matters. Let us call it l_\perp and define it as the weighted average value of $2\pi/k_\perp$:

$$l_\perp = \frac{1}{\langle v^2 \rangle} \int \frac{2\pi}{\sqrt{k_r^2 + k_z^2}} W(k) d^3k = \frac{12\pi^3}{5\langle v^2 \rangle} q C(q) \epsilon^{2/3} k_{\text{inj}}^{-5/3}. \quad (135)$$

Using equation (133), this gives

$$l_{\perp} = \frac{2\pi^2}{5k_{\text{inj}}} . \quad (136)$$

We calculate the effective viscosity as in § 2.2, which gives

$$\nu_* = \frac{1}{3} l_{\perp} \sqrt{\langle v^2 \rangle} = \frac{2\pi^2}{15} \sqrt{6\pi q C(q) \epsilon^{1/3} k_{\text{inj}}^{-4/3}} . \quad (137)$$

If l_{\perp} is the meridional size of these largest eddies, their turnover time is

$$\tau_{\text{turn}} = \frac{l_{\perp}}{\sqrt{\langle v^2 \rangle}} . \quad (138)$$

We can think of several other characteristic times. First the rotation time

$$\tau_{\text{rot}} = \frac{2\pi}{\Omega} ; \quad (139)$$

second, the Alfvén detuning time, which is the time it takes an eddy to be destroyed because its extremities propagate at different Alfvén speeds. Since the cells are anisotropic, one should consider two different Alfvén times, an azimuthal one

$$\tau_{\text{Alf}\theta} = \frac{l_{\parallel}}{l_{\perp} |\nabla(v_{A\theta})|} , \quad (140)$$

and a poloidal one

$$\tau_{\text{AlfP}} = \frac{l_{\perp}}{l_{\perp} |\nabla(\sqrt{\langle v_{\text{AP}}^2 \rangle})|} . \quad (141)$$

The magnitude of the azimuthal field B_{θ} can be estimated by noting that its rate of creation by differential rotation from the radial component, typically $\langle B_r^2 \rangle^{1/2}$, is balanced by its rate of dissipation by effective magnetic diffusivity. Since the poloidal motions alone do not change B_{θ} , the relevant time for turbulence to change this component is $l_{\parallel}/\langle v^2 \rangle^{1/2}$, which is of order of $l_{\parallel}/\langle v^2 \rangle^{1/2}$, and so

$$\Omega \sqrt{\langle B_r^2 \rangle} \approx \sqrt{\langle v^2 \rangle} (B_{\theta}/l_{\parallel}) . \quad (142)$$

This is only valid insofar as the θ -component of the magnetic field is not energetically dominant over the turbulent kinetic energy, which, judging from Brandenburg et al.'s (1995) simulation, is in fact not very well satisfied. Still, accepting this as an estimate only, we find that

$$B_{\theta} \approx \sqrt{\langle B_r^2 \rangle} \frac{\Omega l_{\parallel}}{\sqrt{\langle v^2 \rangle}} . \quad (143)$$

For l_{\parallel} of order r , the local radius, and $\langle v^2 \rangle^{1/2}$ comparable to the sound speed, itself of order ΩH , it is seen that B_{θ} grows much larger than the random poloidal field. This is indeed seen in Brandenburg et al.'s (1995) calculations. From equation (143), we find

$$\tau_{\text{Alf}\theta} \approx \frac{1}{\Omega} \sqrt{\frac{\langle v^2 \rangle}{(\langle B_r^2 \rangle / \mu_0 \rho)}} . \quad (144)$$

Since the poloidal part of the field is not very far from equipartition, the azimuthal Alfvén time is of the order of τ_{rot} . The poloidal Alfvén time is of order

$$\tau_{\text{AlfP}} \approx \frac{1}{\Omega} \frac{\Omega l_{\perp}}{\sqrt{\langle v^2 \rangle}} \sqrt{\frac{\langle v^2 \rangle}{(\langle B_r^2 \rangle / \mu_0 \rho)}} , \quad (145)$$

and it can also be comparable to τ_{rot} . The Rossby number of the turbulence at this scale, which is proportional to the ratio of the rotation time to the eddy turnover time, is

$$\text{Ro} = \frac{1}{2\Omega\tau_{\text{turn}}} = \frac{1}{4\pi} \frac{\tau_{\text{rot}}}{\tau_{\text{turn}}} = \frac{1}{2} \frac{H}{l_{\perp}} \frac{\sqrt{\langle v^2 \rangle}}{c_s} . \quad (146)$$

For slightly subsonic turbulence, the Rossby number may become somewhat smaller than unity. So our assumption that the eddy turnover time is no larger than the rotation time is satisfied only marginally, as has been pointed out before (Dubrulle 1992). However, the consequences of this are less dramatic for MHD turbulence, which still has a direct energy cascade in

two-dimensions, than they are for purely hydrodynamical turbulence. Similarly, we estimate

$$\frac{\tau_{\text{Alfvén}}}{\tau_{\text{turn}}} = \sqrt{\frac{\langle v^2 \rangle}{(\langle B_r^2 \rangle / \mu_0 \rho)}} . \quad (147)$$

For MHD turbulence approaching equipartition for the poloidal components, this ratio approaches unity, and again our assumption of a shorter eddy turnover time is marginal. Hawley et al. (1995) find that the turbulence in their simulation is very near equipartition, sometimes even slightly sub-Alfvénic, and Brandenburg et al. (1995) also find quasi equipartition for poloidal components, but not for toroidal ones. It is found then that the nonlinear transfer time can be regarded as being of order of the turnover time of poloidal eddies. It is possible to express this transfer time from the spectrum itself by the following argument. In modified wavevector space, the turbulence spectrum looks almost isotropic, with a spectral energy $\bar{E}(K)dK$ between K and $K + dK$. From equations (14) and (134),

$$\bar{E}(K) = 4\pi q C(q) \epsilon^{2/3} K^{-5/3} . \quad (148)$$

In the inertial range, this energy is transferred with a flux $\epsilon(K)$, which satisfies a conservation equation

$$\frac{\partial \bar{E}}{\partial t} + \frac{\partial \epsilon}{\partial K} = 0 . \quad (149)$$

In a stationary state, $\epsilon(K)$ reduces to a constant ϵ . Equation (149), however, is useful to show that, in order of magnitude, the nonlinear transfer time τ_{trans} is about

$$\tau_{\text{trans}} \approx \frac{\bar{E}K}{\epsilon} = 4\pi q C(q) \epsilon^{-1/3} K^{-2/3} . \quad (150)$$

The characteristic velocity of eddies of poloidal size $2\pi/K$ is obtained by integrating the spectrum from K to infinity, which gives

$$\langle v_K^2 \rangle = \int_K^\infty W(k) d^3k = \frac{12\pi}{5} q C(q) \epsilon^{2/3} K^{-2/3} . \quad (151)$$

From this, we obtain the nonlinear transfer time as expressed in equation (15) of the paper. Taking $4\pi q C(q) = 1$, the effective viscosity can be obtained in the way described in § 2.2. This gives for v_* the result shown in equation (18), which happens to be of the form of equation (4), with a value of the dimensionless parameter λ given, for this anisotropic turbulence, as in equation (19).

REFERENCES

- Agapitou, V., & Papaloizou, J. C. B. 1985, presented at NATO Advanced Study Institute on Solar and Astrophysical MHD flows, Heraklion, Greece (June 1995)
- Balbus, S. A., & Hawley, J. F. 1991, *ApJ*, 376, 214
- . 1992, *ApJ*, 400, 610
- Bardou, A., & Heyvaerts, J. 1996, *A&A*, 307, 1009
- Blandford, R. D., & Payne, D. G. 1982, *MNRAS*, 199, 88
- Brandenburg, A., Nordlund, A., Stein, R. F., & Torkelsson, U. 1995, *ApJ*, 446, 741
- Canuto, V. M., Goldman, I., & Chasnov, J. 1987, *Phys. Fluids*, 30, 339
- Courant, R., & Hilbert, D. 1937, *Methods of Mathematical Physics* (New York: Wiley-Interscience)
- Dubrule, B. 1992, *A&A*, 266, 592
- Dubrule, B., & Knobloch, E. 1992, *A&A*, 256, 673
- Dubrule, B., & Valdetarro, L. 1992, *A&A*, 263, 387
- Duschl, W. J. 1989, *A&A*, 225, 105
- Ferreira, J., & Pelletier, G. 1993a, *A&A*, 276, 625
- . 1993b, *A&A*, 276, 637
- . 1995, *A&A*, 295, 807
- Fiedler, R. A., & Mouschovias, T. C. 1992, *ApJ*, 391, 199
- Foglizzo, T. 1994, Thèse de Doctorat, Université Paris
- Foglizzo, T., & Tagger, M. 1994, *A&A*, 287, 297
- Fyfe, D., Joyce, G., & Montgomery, D. 1977, *J. Plasma Phys.*, 17, 317
- Goldman, I., & Wandel, A. 1995, *ApJ*, 443, 187
- Hawley, J. F., & Balbus, S. A. 1991, *ApJ*, 376, 223
- Hawley, J. F., Gammie, C. F., & Balbus, S. 1995, *ApJ*, 440, 742
- Heyvaerts, J. 1990, in *IAU Symp. 142, Basic Plasma Processes on the Sun*, ed. E. R. Priest & V. Krishan (Dordrecht: Kluwer), 207
- Heyvaerts, J., & Priest, E. R. 1992, *ApJ*, 390, 297
- Horne, K. 1990, in *IAU Coll. 129, Structure and Emission Properties of Accretion Disks*, ed. C. Bertout, S. Collin Souffrin, J. P. Lasota, & J. Tran Thanh Van (Gif-sur-Yvette: Editions Frontières), 3
- Inverarity, G. W., Priest, E. R., & Heyvaerts, J. 1995, *A&A*, 293, 913
- Jackson, J. D. 1975, *Classical Electrodynamics* (2d ed.; New York: Wiley)
- Kraichnan, R. H., & Montgomery, D. C. 1980, *Rep. Prog. Phys.*, 43, 547
- Lepeltier, T., & Aly, J. J. 1996, *A&A*, 306, 645
- Lin, D. N. C., & Papaloizou, J. C. B. 1980, *MNRAS*, 191, 37
- Lizano, S., & Shu, F. H. 1989, *ApJ*, 342, 834
- Lubow, S. L., Papaloizou, J. C. B., & Pringle, J. E. 1994, *MNRAS*, 267, 235
- Lubow, S. L., & Spruit, H. C. 1995, *ApJ*, 445, 337
- Marsh, T. R., Horne, K., Schlegel, E. M., Honeycutt, K., & Kaitchuck, R. H. 1990, *ApJ*, 364, 637
- Matthaeus, W. H., & Montgomery, D. 1980, in *Non Linear Dynamics*, ed. R. H. G. Helleman (Ann. NY Acad. Sci., Vol. 357), 203
- Mestel, L. 1966, *MNRAS*, 133, 265
- Mestel, L., & Spitzer, L. 1956, *MNRAS*, 116, 504
- Mestel, L., & Strittmatter, P. A. 1967, *MNRAS*, 137, 95
- Moffat, H. K. 1983, *Rep. Prog. Phys.*, 46, 621
- Mouschovias, T. C. 1995, in *The Physics of the Interstellar medium*, ed. A. Ferrara, C. Heiles, C. F. McKee, & S. Shapiro (San Francisco: ASP), in press
- Mouschovias, T. C., & Morton, S. A. 1992, *ApJ*, 390, 144
- Nakano, T. 1979, *PASJ*, 31, 697
- Norman, C. A., & Heyvaerts, J. 1985, *A&A*, 147, 247
- Parker, E. N. 1983, *ApJ*, 264, 642
- Pouquet, A., Frisch, U., & Léorat, J. 1976, *J. Fluid Mech.*, 77, 321
- Pringle, J. E. 1981, *ARA&A*, 19, 137
- Pudritz, R. E. 1981, *MNRAS*, 195, 897
- Pudritz, R. E., & Norman, C. A. 1983, *ApJ*, 274, 677
- Sakimoto, P. J., & Coroniti, F. V. 1989, *ApJ*, 342, 49
- Shakura, N., & Sunyaev, R. 1973, *A&A*, 24, 337
- Spruit, H. C., Stehle, R., & Papaloizou, J. C. B. 1995, *MNRAS*, 275, 1223
- Spruit, H. C., & Taam, R. E. 1990, *A&A*, 229, 475
- Stella, L., & Rosner, R. 1984, *ApJ*, 277, 312
- Stepinsky, T. F., & Levy, E. H. 1989, *ApJ*, 350, 819
- Stone, J. M., Hawley, J. F., Gammie, C. F., & Balbus, S. A. 1996, *ApJ*, 463, 656
- Tagger, M., Henriksen, R. N., Sygnet, J. F., & Pellat, R. 1990, *ApJ*, 353, 654
- Torkelsson, U. 1993, *A&A*, 274, 675
- van Ballegooijen, A. A. 1986, *ApJ*, 311, 1001
- Zahn, J. P. 1991, in *IAU Colloq. 129, Structure and Emission Properties of Accretion Disks*, ed. C. Bertout, S. Collin Souffrin, J. P. Lasota, & J. Tran Thanh Van (Gif-sur-Yvette: Editions Frontières), 87